NASA TECHNICAL NOTE

NASA TN D-5336

NASA TN D-5336

GASEOUS-HYDROGEN REQUIREMENTS FOR THE DISCHARGE OF LIQUID HYDROGEN FROM A 1.52-METER- (5-FT-) DIAMETER SPHERICAL TANK

by Robert J. Stochl, Philip A. Masters, Richard L. DeWitt, and Joseph E. Maloy

Lewis Research Center
Cleveland, Ohio

NATIONAL AERONAUTICS AND SPACE ADMINISTRATION • WASHINGTON, D. C. • AUGUST 1969

GASEOUS-HYDROGEN REQUIREMENTS FOR THE DISCHARGE OF LIQUID HYDROGEN FROM A 1.52-METER- (5-FT-) DIAMETER SPHERICAL TANK

By Robert J. Stochl, Philip A. Masters, Richard L. DeWitt, and Joseph E. Maloy

Lewis Research Center
Cleveland, Ohio

NATIONAL AERONAUTICS AND SPACE ADMINISTRATION

For sale by the Clearinghouse for Federal Scientific and Technical Information
Springfield, Virginia 22151 – CFSTI price $3.00

ABSTRACT

An experimental investigation was conducted to determine the effect of various physical parameters on the pressurant gas requirements during the pressurization and expulsion of liquid hydrogen from a 1.52-m- (5-ft-) diameter spherical tank. The experimental results were compared with results predicted by an analytical program. Tests were conducted for a range of outflow rates at a nominal operating pressure level of 34.47×10^4 N/m^2 (50 psia) using inlet gas temperatures of 167, 298, and 355 K (301°, 536°, and 639° R). Data were obtained using three pressurant injector geometries (hemisphere, radial, and straight pipe) and two tank wall thicknesses (0.762 and 0.409 cm; 0.30 and 0.161 in.). The experimental results indicate that the inlet gas temperature has the strongest influence on the pressurant gas requirements followed closely by the influence of injector geometry. Fair agreement existed between the analysis and experimental data when using a diffuser-type (hemisphere and radial) injector. The agreement between the experimental data and the analysis was not good when using the straight pipe injector.

GASEOUS-HYDROGEN REQUIREMENTS FOR THE DISCHARGE OF LIQUID HYDROGEN FROM A 1.52-METER- (5-FT-) DIAMETER SPHERICAL TANK

by Robert J. Stochl, Philip A. Masters, Richard L. DeWitt, and Joseph E. Maloy

Lewis Research Center

SUMMARY

An experimental investigation was conducted to determine the effect of various physical parameters on the pressurant gas requirements during the pressurization and expulsion of liquid hydrogen from a 1.52-meter- (5-ft-) diameter spherical tank. Tests were conducted for a range of outflow rates at a nominal operating pressure level of 34.47×10^4 newtons per square meter (50 psia) using inlet gas temperatures of 167, 298, and 355 K (301°, 536°, and 639° R). Data were obtained using three pressurant injector geometries (hemisphere, radial, and straight pipe) and two tank wall thicknesses (0.762 and 0.409 cm; 0.30 and 0.161 in.).

The experimental results indicate that the inlet gas temperature has the strongest influence on the pressurant gas requirements followed closely by the influence of injector geometry. Results also indicate that tank wall thickness does not greatly influence the pressurant gas requirements.

The experimental results were compared with results predicted by a previously developed analytical program which was revised and extended for the test conditions. Fair agreement existed between the analysis and experimental data when using a diffuser-type injector. The agreement between experimental data and the analysis was not as good when using the straight pipe injector.

INTRODUCTION

During the past several years, a great deal of effort has been devoted to the problems associated with the pressurized discharge of a cryogenic liquid from a tank. The main objectives of these efforts have been toward the optimization of a propellant tank pressurization system. One phase of this optimization is a precise determination of pressurant requirements for any given set of operating parameters (e.g., tank pressure,

inlet gas temperature, liquid flow rate, etc.). This knowledge would allow the design of a system that carried only the weight of gas necessary to accomplish the mission.

Several investigators have developed analyses (e.g., refs. 1 and 2) which attempt to predict the pressurant gas requirements during the pressurized discharge of a cryogenic fluid. These analyses, however, are either burdened with simplifying assumptions or involve parameters and terms about which little is generally known "a priori." Because of these limitations the validity of the analytical results has to be verified largely by correlations of experimental results.

Therefore, an investigation was conducted at the Lewis Research Center to determine experimentally the effect of various physical parameters (e.g., tank geometry and size, injector geometry, pressurant gas, inlet gas temperature, etc.) on the pressurant gas requirements during the expulsion of liquid hydrogen from propellant tanks. The information obtained could be used in the design of optimum pressurization systems for particular missions. The results of this investigation were also used to determine the capability of the analysis of reference 1 to predict the pressurant gas requirements for the various physical parameters. Although the analysis of reference 2 is widely used in the design and analysis of pressurization systems, its use requires values for many empirical constants and physical parameters. In many cases these values must be obtained from experimental data on prototype systems. Inasmuch as these constants and parameters were not available, it was decided to use the analysis of reference 1 since it required the least amount of prior knowledge of a particular system.

Small scale test work was done in a 0.82 cubic meter (29 ft^3) cylindrical tank to determine the effect of injector geometry on the pressurant gas requirements (GH_2) during the dischange of liquid hydrogen (LH_2). The results of this work are reported in reference 3. The analysis, for this case, proved to be adequate (within ±10 percent) in predicting the pressurant gas requirements even though two of its major assumptions were shown to be invalid - namely, no heat transfer to the liquid surface, and no mass transfer.

This report presents the results obtained in 1.52-meter- (5-ft-) diameter spherical aluminum tanks. The primary objective of these tests was to obtain additional experimental information on the pressurant requirements during the initial pressurization as well as the expulsion period in larger scale tanks for the various operation parameters. Information was also obtained on tank wall heating, liquid heating, residual ullage energy, and mass transfer in order to gain an insight into the reasons for any variations in pressurant gas requirements. An additional objective was to compare the experimental results with the predicted ones.

For this report the analysis of reference 1 was revised and extended (as described in appendixes A and B) to account for energy transfer occurring at the gas-liquid interface in tanks of any arbitrary symmetric tank shape. The analysis was also modified and extended (as described in appendix C) to cover the initial pressurization period. The

major limiting assumptions still remaining from the original analysis are one-dimensional flow and no mass transfer. Although reference 3 showed the inadequacy of these assumptions when analyzing a straight pipe injector, a more rigorous analysis was not attempted because of the added complexity.

The tests reported herein were conducted in a vacuum chamber using 1.52-meter-(5-ft-) diameter spherical aluminum tanks. The main test variables were as follows:

Tank wall thickness, cm (in.)	0.762 and 0.409 (0.30 and 0.161)
Pressurant gas injector geometry	hemisphere, radial, and straight pipe
Nominal inlet gas temperature, K (^{o}R)	167, 298, and 355 (301, 536, and 639)
Liquid outflow rates, kg/sec (lb/sec)	between 0.859 and 0.218 (1.890 and 0.481)
Initial gas ullages in tank, percent	4, 28, 55, and 75

The high outflow rate corresponds to a tank expulsion time of 132.4 seconds and a thrust level of 2290 kilograms (5050 lb). The expulsion time and thrust level corresponding to the low flow rate are 531.9 seconds and 580 kilograms (1280 lb). The thrust levels are based on a specific impulse of 444 seconds and an oxidant to fuel ratio (O/F) of 5. Data were also obtained for pressurization of the tank at various rates (6.48×10^{3} to 2.65×10^{4} $(N/m^{2})/sec$; 0.94 to 3.85 psi/sec) from 1 atmosphere to the desired operating level. All tests were performed using gaseous hydrogen as a pressurant at a nominal operating tank pressure of 34.47×10^{4} newtons per square meter (50 psia).

SYMBOLS

A	area, m^{2} (ft^{2})
b	$1 - \frac{Z_1}{Z} - 2\frac{\Delta r}{r}$
C	orifice coefficient
C_H	effective perimeter of interior hardware, m (ft)
C_p	specific heat at constant pressure, J/(kg)(K) (Btu/(lb)(^{o}R))
C_v	specific heat at constant volume, J/(kg)(K) (Btu/(lb)(^{o}R))
C_w	specific heat of tank wall, J/(kg)(K) (Btu/(lb)(^{o}R))
c	$\alpha - (\alpha\omega) - T_w - \left(\frac{1}{l_w \rho_w}\right)(\Delta t)\frac{\dot{q}}{C_w}$
D	orifice diameter, m (ft)

d	$\left(\frac{Z_2}{Z}\right)\left(\frac{\Delta x}{\Delta t}\right)\left(\frac{P' - P}{P'}\right) - \left(\frac{Z_1}{Z}\right)\left(\frac{\Delta x}{\Delta t}\right)$
Gr	Grashof number, $\frac{L^3\rho^2 g\ \Delta T\beta}{\mu^2}$
g	gravity acceleration, m/sec^2 (ft/sec^2)
H	enthalpy, J (Btu)
h	specific enthalpy, J/kg (Btu/lb)
h_c	convective heat-transfer coefficient, $J/(m^2)(K)(sec)$ $(Btu/(ft^2)(^oR)(sec))$
k	thermal conductivity, $J/(m)(K)(sec)$ $(Btu/(ft)(^oR)(sec))$
L	flow length, m (ft)
l	thickness, m (ft)
M	mass, kg (lb)
ΔM	differential mass, kg (lb)
$\dot{M}$	mass flow rate, kg/sec (lb/sec)
$\overline{M}$	molecular weight, kg/(kg)(mole) (lb/(lb)(mole))
M_{GN}	net mass added to ullage, $M_G \pm M_t$, kg (lb)
M_I	ideal pressurant requirement, kg (lb)
N	number of volume segments
Nu	Nusselt number, h_cL/k
n (or i)	summing index
P	pressure, N/m^2 $(lb/in.^2)$
Pr	Prandtl number, $\mu C_p/k$
Δp	differential pressure, N/m^2 $(lb/in.^2)$
Δp^*	orifice Δp
Q	heat transfer, J (Btu)
$\dot{Q}$	heat-transfer rate, J/sec (Btu/sec)
$\dot{Q}'$	specific heat-transfer rate, J/(kg)(sec) (Btu/(lb)(sec))
$\dot{q}$	heat-transfer rate per unit area, $J/(m^2)(sec)$ $(Btu/(ft^2)(sec))$
R	gas constant, J/(K)(mole)
Re	Reynolds number, $\rho L\overline{V}/\mu$

r	radius, m (ft)
Δr	increment of radius, m (ft)
T	temperature, K (^{o}R)
ΔT	differential temperature, K (^{o}R)
T_{δ}	temperature at the edge of thermal boundary layer, K (^{o}R)
t	time, sec
Δt	time increment, sec
U	internal energy, J (Btu)
ΔU	differential energy, J (Btu)
u	specific internal energy, J/kg (Btu/lb)
V	volume, m^3 (ft^3)
ΔV	volume increment, m^3 (ft^3)
$\overline{V}$	velocity, m/sec (ft/sec)
v	specific volume, m^3/kg (ft^3/lb)
W	work, J (Btu)
X_n	number of volume elements in the ullage
x	coordinate in direction of tank axis, m (ft)
Δx	space increment, m (ft)
Y	expansion factor
y	thickness within the boundary layer, m (ft)
Z	compressibility factor, $Z = pv/RT$
z	elevation or vertical distance along tank wall, m (ft)
α	$\dfrac{1 + \left(\dfrac{h_c \Delta t}{l_w \rho_w C_w}\right)}{\left(\dfrac{2h_c RZ \Delta t}{r\overline{M}C_p P}\right)\left[1 + \left(\dfrac{\Delta r}{\Delta x}\right)^2\right]^{1/2}}$
β	coefficient of thermal expansion, $1/K$ ($1/^{o}R$)
γ	specific heat ratio
δ	finite increment, or total boundary layer thickness, m (ft)

λ	latent heat of vaporization, J/kg (Btu/lb)
μ	viscosity, kg/(m)(hr) (lb/(ft)(hr))
ρ	density, kg/m^3 (lb/ft^3)
ω	$\left(\frac{R}{M} Z_1 \frac{\Delta p}{\Delta t} + \frac{RZ}{\overline{M} \pi r^2} \dot{Q}'_H\right)\frac{\Delta t}{C_p P}$

Subscripts:

A	analytical results
ad	adiabatic
E	experimental results
f	final state or condition
G	gas added to tank
H	internal hardware
i	initial state or condition, or i^{th} term
i→f	from initial to final state or condition
L	liquid
o	condition prior to ramp
S	liquid surface
sat	saturation
T	total quantity
t	transferred
U	ullage
w	wall

Superscript:

1	time index

APPARATUS AND INSTRUMENTATION

Facility

All tests were conducted under vacuum inside a 7.61-meter- (25-ft-) diameter spherical vacuum chamber (fig. 1) to reduce the external convective heat transfer into the pro-

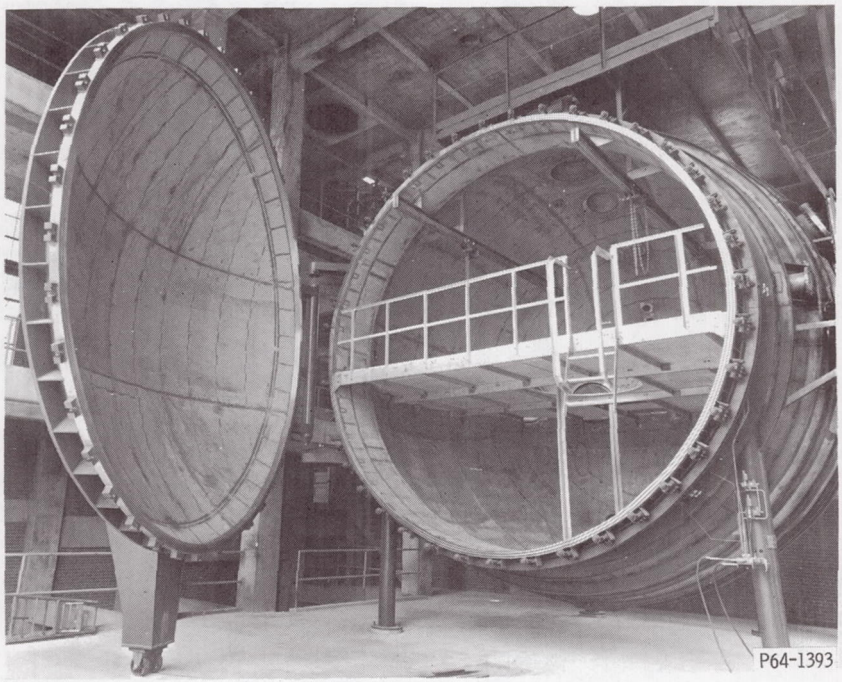

Figure 1. - 7.61-Meter- (25-ft-) diameter vacuum chamber.

pellant tank. The vacuum capability of this chamber was approximately 8×10^{-7} millimeter of mercury. A general schematic of the test tank and associated equipment is shown in figure 2. A heat exchanger and blend valve subsystem capable of delivering gaseous hydrogen at temperatures of 167 to 405 K (301° to 729° R) at a maximum flow rate of 5.40×10^{-2} kilogram per second (0.12 lb/sec) were used to control pressurant gas inlet temperature. A ramp generator and control valve were used for controlling the initial rate of pressurization of the propellant tank. A closed-loop pressure control circuit was used to maintain constant tank pressure during the expulsion period. The liquid outflow rate was controlled by remotely operated variable flow valves. The liquid hydrogen outflow from the tank was returned to the storage Dewar.

Liquid outflow rates were measured using a turbine-type flowmeter located in the transfer line. The flowmeter was calibrated (within an estimated uncertainty of ±1/2 percent) with liquid hydrogen over the expected range of flow rates. The calibration was performed at Lewis Research Center. Pressurant gas inlet flow rates were determined by the use of an orifice located in the pressurant supply line. Tank, line, and differential pressures were measured with bonded strain-gage-type transducers (estimated uncertainty of ±1/4 percent).

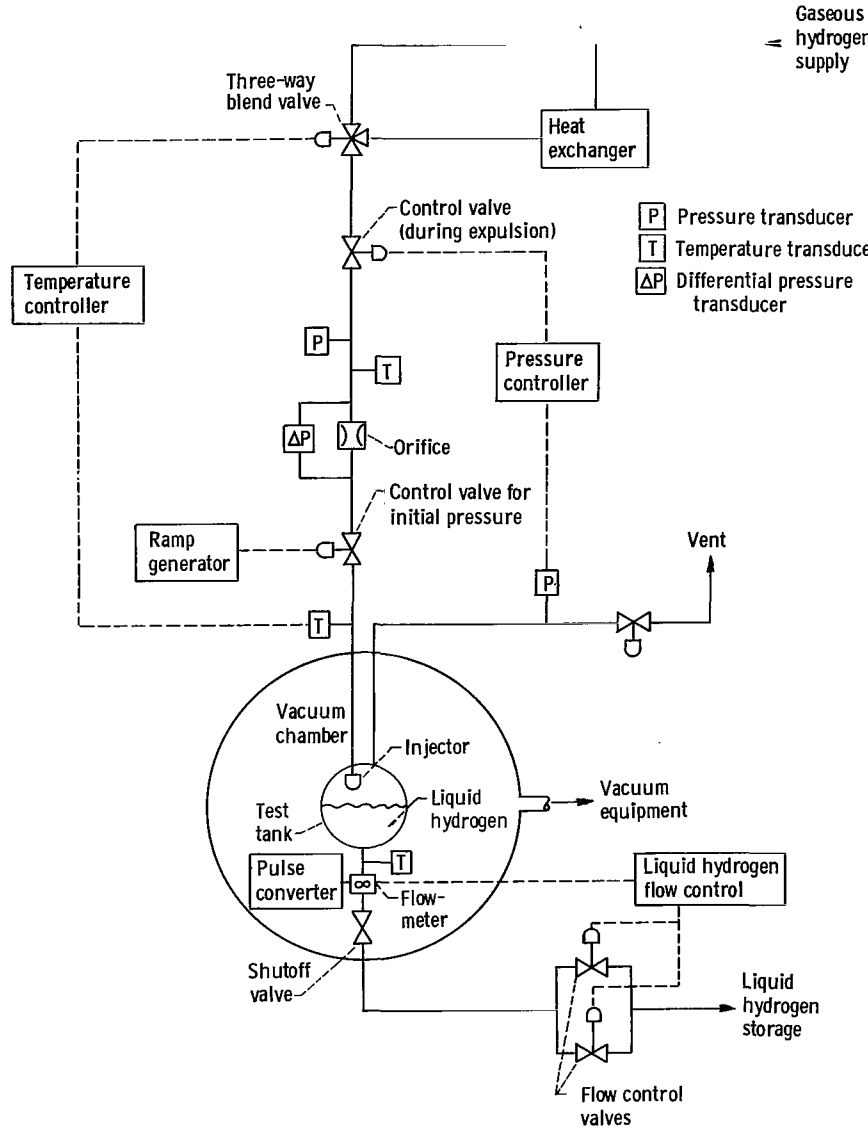

Figure 2. - General schematic of facility.

Test Tanks

The experimental work was conducted in 1.52-meter- (5-ft-) diameter bare wall spherical aluminum tanks. One tank (fig. 3) had an average wall thickness of 0.762 centimeter (0.30 in.). The other tank was identical except the wall was chem-milled down to an average thickness of 0.409 centimeter (0.161 in.). One stainless steel lid served both tanks. The lid housed the inlet and vent pipes and the electrical connections for all internal tank instrumentation. The lid was 0.457 meter (18 in.) in diameter, 3.18 centimeters

Figure 3. - 1.52-Meter- (5-ft-) diameter spherical test tank. Tank wall thickness, 0.762 centimeter (0.30 in.).

(1.25 in.) thick, and weighed 67.50 kilograms (149 lb). The inner surface of the lid conformed to the contour of the tank wall.

A view port and television camera were installed on the 0.762-centimeter (0.30-in.) wall test tank (fig. 4) for the purpose of visually locating the initial liquid in the tank prior to expulsion and to enable observation of any physical processes occurring in the tank. Lighting the tank interior was accomplished by bulbs mounted on the inner surface of the tank wall.

Pressurant Gas Injector Geometries

The three injector geometries tested are shown in figure 5. These particular geometries were selected because they represent the three basic injection patterns of reference 3. The hemisphere injector diffuses the pressurant uniformly in all directions into the ullage volume. The radial injector injects the pressurant gas radially toward the tank wall. And the straight pipe injects the pressurant gas in a concentrated jet toward the liquid surface. The hemisphere and radial injectors, which best seem to conform to the analytical assumption of one-dimensional gas flow as shown in reference 3, have approximately the same open exit area for the hemisphere (176.8 cm^2; 27.4 $in.^2$) and for

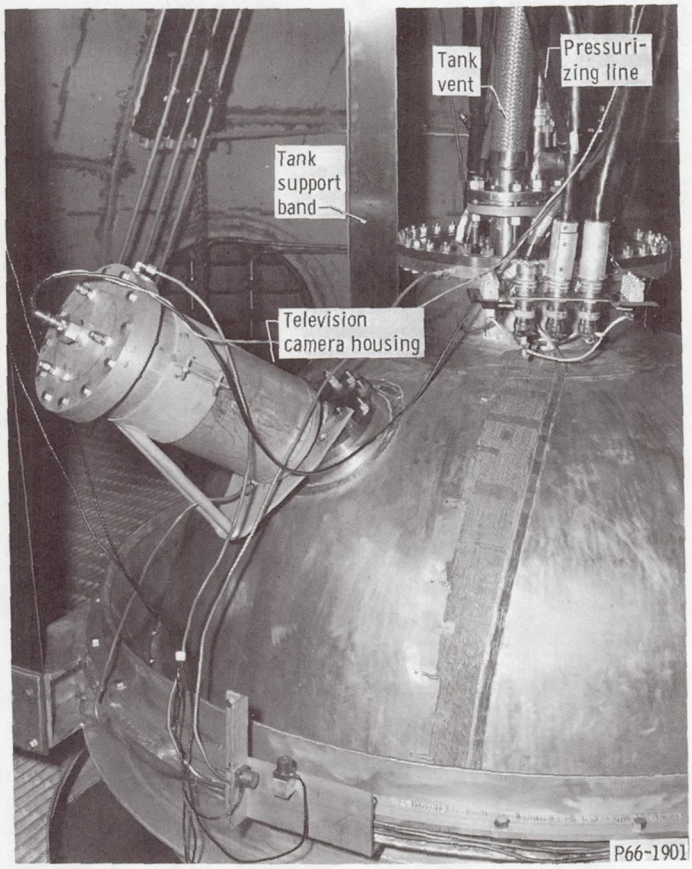

Figure 4. - View port and television camera installation on test tank. Wall thickness, 0.762 centimeter (0.30 in.).

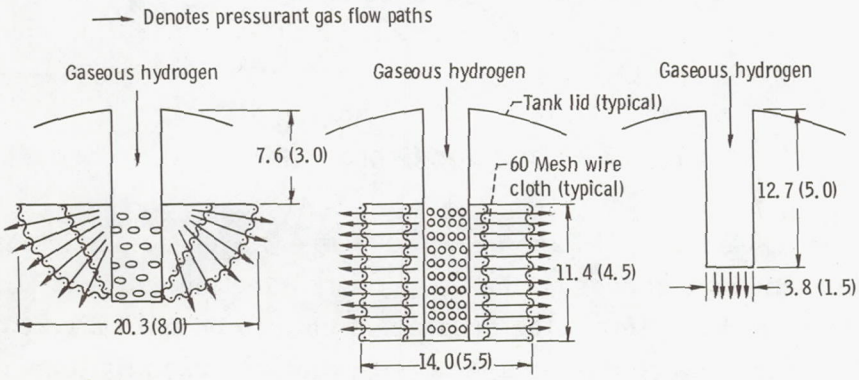

(a) Hemisphere injector. Open area, 176.8 square centimeters (27.4 in.^{2}).

(b) Radial injector. Open area, 170.3 square centimeters (26.4 in.^{2}).

(c) Straight pipe injector. Open area, 9.5 square centimeters (1.47 in.^{2}).

Figure 5. - Injector geometries. All dimensions are in centimeters (in.).

the radial injector (170.3 cm^2; 26.4 $in.^2$). The straight pipe injector had an open area of 9.5 square centimeters (1.47 $in.^2$).

Internal Tank Instrumentation

Ullage gas temperatures were used to determine the mass and energy content of the tank ullage. These temperatures must be obtained with sensors capable of accurate measurement of rapid changes in temperature. Internal tank instrumentation is illustrated in figure 6. Location of the vertical and horizontal ullage gas temperature rakes are indicated. The thermopile was the basic temperature measurement technique used in this investigation. The use of thermopiles to measure ullage gas temperature was first developed in reference 4, and the technique was used with good results in reference 3. The main advantage of using thermopiles is their fast response time (between 0.2 and 1.0 sec) in going from saturated liquid to saturated vapor. This time response is approximately an order of magnitude less than sensors generally used in this type of investigation.

A typical three-element thermopile unit and its associated wiring schematic are illustrated in figure 7(a). The thermopile units were constructed of 0.202 millimeter

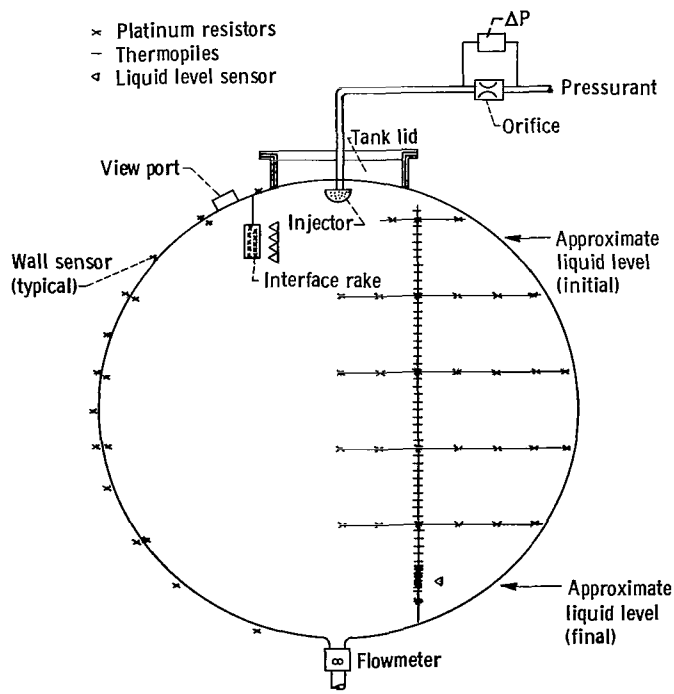

Figure 6. - 1.52-Meter- (5-ft-) diameter test tank.

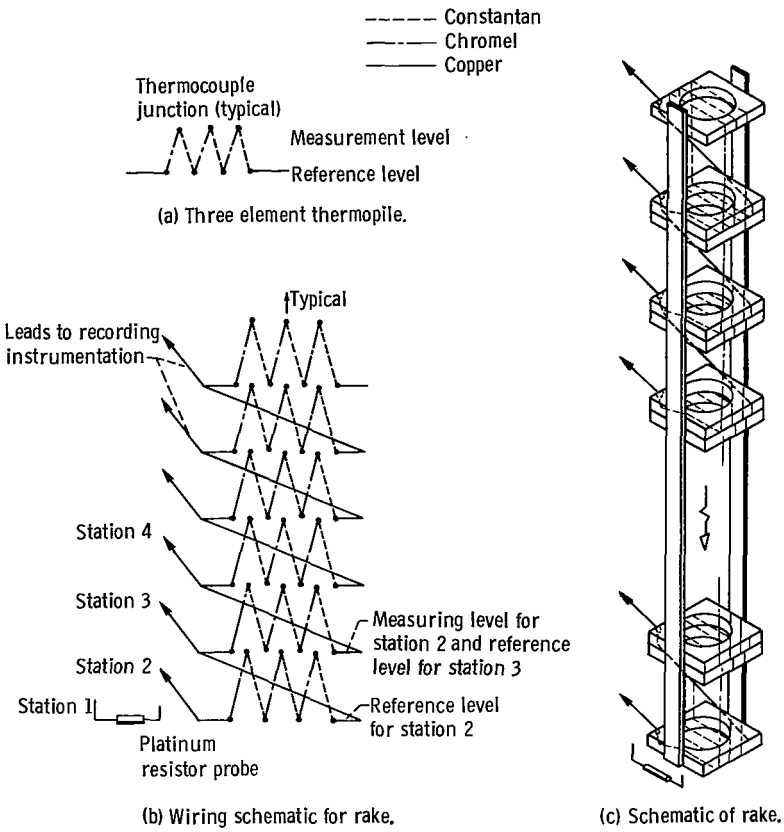

Figure 7. - Thermopile rake.

chromel and constantan wire. The support structure was made of Bakelite to minimize thermal conduction from one measurement station to another. Vertical ullage gas temperature profiles were obtained by stacking the individual thermopile units as shown in figures 7(b) and (c). The spacing between the reference and measuring levels was 2.54 centimeters (1.0 in.) for the top 45 thermopiles composing the vertical rake. The 10 units at the bottom of the rake had a 1.27-centimeter (0.50-in.) spacing in order to obtain a more accurate temperature profile of the ullage gas near the liquid surface at the end of an expulsion.

Platinum resistance sensors, which were located at least every tenth station starting from the bottom of the rake, sensed the absolute temperature at their location and provided a reference for the thermopiles above the location. The horizontal rakes were composed of platinum resistance sensors spaced a maximum of 12.70 centimeters (5.00 in.) apart in the radial direction. Two platinum resistance sensors were used at each location to measure liquid and/or gas temperatures in the ranges 20 to 38.9 K (36° to 70° R) and 38.9 to 277.8 K (70° to 500° R). These dual sensors permitted more accurate

measurements of liquid and gas temperatures than could be achieved with one sensor covering the entire range.

The initial static temperature profile near the liquid surface was determined by a fixed interface rake. This rake contained 13 platinum resistance sensors spaced 0.64 centimeter (0.25 in.) apart. The range of these sensors was 20 to 38.9 K (36° to 70° R). For complete tank expulsions (i.e., 5 percent ullage to 5 percent outage), the initial liquid level was always assured to be on the interface rake in the thick walled tank by monitoring a closed-circuit television system which viewed, through a port in the tank, the position of the liquid-gas interface on a scale fixed to the interface rake (fig. 6). For tests conducted at the 28, 55, and 75 percent ullage values, the scale was moved lower in the tank and the television camera was refocused. The liquid level for the thin-walled tank was determined by hot-wire liquid level sensors located on the interface rake.

Platinum resistance sensors were also used to determine tank wall temperatures at twelve locations and the liquid temperature at the flowmeter. Copper-constantan thermocouples were used to determine tank lid temperatures at five locations and the pressurant gas inlet temperature.

All measurements were recorded on a high-speed digital data system. The measurements were recorded at a rate of 3.125×10^3 channels per second. Each measurement channel was sampled every 0.064 second.

PROCEDURE

The spherical test tank was filled from the bottom to approximately a 2 percent ullage condition. It was then topped off as necessary while the tank lid and peripheral support hardware reached steady-state operating temperatures.

Temperature conditioning of the pressurant gas was then started. Gas flow was established through the heat exchanger loop, through the control valves and orifice arrangement, and then into the tank ullage from which it was vented through the conditioning line to the outside as shown in figure 2. The temperature control circuit shown in figure 2 was used to get the desired pressurant gas temperatures during the flow period. When the pressurant gas temperature conditioning was almost completed, the liquid level in the test tank was adjusted to a desired value by either topping or slow draining. The liquid level was observed on closed-circuit television for the thick-wall tank. Liquid level, for the thin-wall tank, was located by the use of hot-wire liquid level sensors. The pressurant gas flow was then stopped and the test tank was vented in preparation for an expulsion run. The automatic controllers and timers were preset with all the desired run and operating conditions (i.e., tank pressure level, length of ramp period, length of hold period, liquid outflow valve position, start and stop times of the data recording equipment, etc.).

After starting the data recording equipment, the next step of the completely automatic run sequence took electrical calibrations on all pressure transducers. Immediately following this, the test tank was pressurized over a predetermined time period to the nominal operating pressure of 34.47×10^4 newtons per square meter (50 psia). Tank pressure was held constant for about 30 seconds to stabilize internal temperatures. The tank expulsion period was then started. Approximately 90 percent of the total tank volume was expelled at a constant volumetric flow rate. The expulsion period was stopped when a hot-wire liquid level sensor located at the 95-percent ullage level indicated gas. The last step of the automatic run sequence was the stopping of all data recording equipment. The test tank was then vented and refilled with liquid hydrogen for the next expulsion.

Additional ramp pressurization runs, with no expulsion, were made for three different tank ullage levels. The only deviation in the operating procedure for these runs was that the liquid outflow value was locked shut. As a result, after the ramp period, the hold period was simply extended as long as was desired.

DATA REDUCTION

Physical Description of Problem

An initially vented tank containing a two-phase one-component cryogenic fluid was pressurized from 1 atmosphere to a new pressure by adding gas. The system was then allowed to reach a new equilibrium condition at which time liquid outflow was started. During this expulsion period, pressurant gas (at constant temperature) was added to the tank at a rate that maintained a constant tank pressure while expelling the liquid at a desired rate. The amount of pressurant gas used during the expulsion phase is dependent on (1) the volume of liquid displaced with no heat or mass transfer, (2) the heat transfer to the tank wall and liquid, and (3) the amount of mass condensed or evaporated.

The main parameter used in the comparisons was the ratio of the ideal pressurant requirement to the actual pressurant requirement. The ideal pressurant wad determined under the assumption that the incoming pressurant gas did not exchange energy or mass with the surroundings. Under this assumption, the ideal pressurant required for the initial pressurization of the tank was determined by the relation

$$M_I = \frac{MP_o V_o}{ZRT_G}\left[\left(\frac{P_f}{P_o}\right)^{1/\gamma} - 1\right] \tag{1}$$

The ideal pressurant required for the expulsion period was determined by the relation

$$M_I = \frac{\overline{MP}\ \Delta V_U}{ZRT_G} \tag{2}$$

Mass Balance

A mass balance was performed on the ullage volume from an initial time t_i to a final time t_f as follows:

$$M_{U,f} = M_{U,i} + M_{G,i \to f} \pm M_{t,i \to f} \tag{3}$$

A discussion of how the terms of equation (3) were determined is now presented.

Pressurant gas added ($M_{G,i \to f}$). - The weight of the actual pressurant gas added from any initial time t_i to any final time t_f was determined by numerical integration of the gas orifice equation

$$M_{G,i \to f} = \int_{t_i}^{t_f} yD^2C\sqrt{\rho\ \Delta p^*}\ dt \tag{4}$$

Note that $(t_f - t_i)$ is the time necessary to expel ΔV_U (m^3) of liquid.

Ullage mass. - The initial ullage mass $M_{U,i}$ and the final ullage mass $M_{U,f}$ were obtained by numerical integration of the particular density profiles as follows:

$$M_{U,i} = \int_{V_{U,i}} \rho\ dV \simeq \sum_{n=1}^{N_i} \rho_n\ \Delta V_n \qquad \text{where } \rho = f(T) \tag{5}$$

$$M_{U,f} = \int_{V_{U,f}} \rho\ dV \simeq \sum_{n=1}^{N_f} \rho_n\ \Delta V_n \qquad \text{where } \rho = f(T) \tag{6}$$

The internal tank volume was considered as 57 (corresponding to thermopile location) horizontal disk segments. Each of these segments was in turn divided radially into a series of concentric rings, the number of which depended on the location of radial temperature sensors and the vertical position of the disk segment being considered. These rings (339 in all) comprised the V_n's in the previous calculations. In this manner, vertical temperatures as well as radial temperature gradients could be incorporated into

the mass calculations. The position of the liquid level prior to and after expulsion determined the number of gas volume rings (N_i and N_f) used in the ullage mass calculations.

Mass transfer. - The mass transfer was calculated from equation (3) as a result of knowing $M_{U,f}$, $M_{U,i}$, and $M_{G,i\rightarrow f}$; that is,

$$M_{t,i\rightarrow f} = M_{U,i} + M_{G,i\rightarrow f} - M_{U,f}$$

If $M_{t,i\rightarrow f}$ was a positive quantity, mass was considered leaving the ullage volume (e.g., condensation).

Energy Balance

For the thermodynamic system consisting of the entire tank and its contents (tank + ullage gas + liquid), the first law of thermodynamics for an increment of time dt may be written as

$$dU_T = (\delta M_G)\left(u_G + P_G v_G + \frac{\overline{V}_G^2}{2g} + Z_G\right) - (\delta M_L)\left(u_L + P_L v_L + \frac{\overline{V}_L^2}{2g} + Z_L\right) + \delta Q - \delta W \qquad (7)$$

The kinetic and potential energy terms are small in comparison with the other energy terms and will be neglected in this development. If $h = u + pv$ is substituted, equation (7) becomes

$$dU_T = (\delta M_G)h_G - (\delta M_L)h_L + \delta Q - \delta W \qquad (8)$$

For this system, there is no external work done on the system so $\delta W = 0$. The final form of equation (7) is

$$dU_T = (\delta M_G)h_G - (\delta M_L)h_L + \delta Q \qquad (9)$$

Equation (9) can be integrated over any time period. The physical interpretation of the quantities in equation (9) is as follows:

$$\int_{U_{t_i}}^{U_{t_f}} dU_T = \int_{t_i}^{t_f} \dot{M}_G h_G \, dt - \int_{t_i}^{t_f} \dot{M}_L h_L \, dt + \int_{t_i}^{t_f} \dot{Q} \, dt \qquad (10)$$

Change in system energy (Tank + gas + liquid)	Energy input by pressurant gas inflow	Energy leaving through liquid outflow	Energy from environment (Heat leak from conduction, convection, and radiation)

The terms of equation (10) were evaluated in the following manner.

Energy input by pressurant gas inflow. - The first term in equation (10) may be evaluated as follows:

$$\int_{t_i}^{t_f} \dot{M}_G h_G \, dt \simeq \sum_{n=0}^{n=(t_f - t_i/\Delta t)} \dot{M}_G h_G \, \Delta t \qquad (11)$$

The pressurant flow rate $\dot{M}_G$ was determined from equation (4). The specific enthalpy of the inlet gas was evaluated at the inlet temperature and pressure at each time increment Δt.

Energy leaving by liquid outflow. -

$$\int_{t_i}^{t_f} \dot{M}_L h_L \, dt \simeq \sum_{n=0}^{n=(t_f - t_i/\Delta t)} \dot{M}_L h_L \, \Delta t \qquad (12)$$

The liquid flow rate $\dot{M}_L$ was determined from the turbine flowmeter. The specific enthalpy of the liquid was evaluated at the outlet temperature.

Energy input from environment. - The rate of energy input into the tank from the environment was assumed to be the same for all cases and was determined from a boiloff test. This test indicated a nominal value of 0.732×10^3 joules per second (0.694 Btu/sec) should be used. This value which includes heat input by radiation, convection, and conduction through pipes and supports was in all test cases less than 7.0 percent of the energy added to the tank by the pressurant gas:

$$\int_{t_i}^{t_f} \dot{Q} \, dt \simeq 0.732 \times 10^3 (t_f - t_i) \qquad (13)$$

Change in system energy. - The change in system energy can be separated into the categories of (1) change in ullage energy, (2) change in liquid energy, and (3) change in the wall energy:

$$dU_T = dU_U + dU_L + dU_w \tag{14}$$

Change in ullage energy. - The change in the ullage energy over any given time interval $(t_i \rightarrow t_f)$ is obtained by subtracting the internal energy of the ullage at time t_i from the internal energy at time t_f:

$$\int_{U_{t_i}}^{U_{t_f}} dU_U = \left(U_U\right)_{t_f} - \left(U_U\right)_{t_i} \tag{15}$$

Making use of the relation $U = H - PV$ gives

$$\int_{U_{t_i}}^{U_{t_f}} dU_U = \sum_{V_f} \rho\left(h - \frac{p}{\rho}\right) \Delta V - \sum_{V_i} \rho\left(h - \frac{p}{\rho}\right) \Delta V \tag{16}$$

The ullage gas density and enthalpy are functions of pressure and temperature. Therefore, by knowing the pressure and temperature profiles at times t_f and t_i one can evaluate the change in ullage energy.

Change in liquid energy. - The change in energy of the liquid in the tank can be determined in a manner similar to the change in ullage energy:

$$\int_{U_{t_i}}^{U_{t_f}} dU_L = \left(U_L\right)_{t_f} - \left(U_L\right)_{t_i} \tag{17}$$

or

$$\int_{U_{t_i}}^{U_{t_f}} dU_L = \sum_{V_f} \rho_L\left(h_L - \frac{p}{\rho_L}\right) \Delta V - \sum_{V_i} \rho_L\left(h_L - \frac{p}{\rho_L}\right) \Delta V \tag{18}$$

Here again the liquid density and enthalpy are functions of pressure and temperature.

Change in wall energy. - The change in wall energy was determined by applying the first law of thermodynamics to an element of the wall:

$$\int_{U_{t_i}}^{U_{t_f}} dU_w = \Delta U_w = \Delta M_w \int_{T_1}^{T_2} C_v \, dT \qquad \text{where } C_v = C_v(T) \tag{19}$$

The total change of the wall is then

$$\Delta U_{w,T} = \sum^{M_w} (\Delta U_w)_n = \sum^{M_w} \Delta M_w \int_{T_1}^{T_2} C_v(T) \, dT \tag{20}$$

For convenience, equation (14) is substituted into equation (10):

$$\int_{t_i}^{t_f} \frac{d}{dt}\left(U_u + U_w + U_L\right) dt = \int_{t_i}^{t_f} \dot{M}_G h_G \, dt - \int_{t_i}^{t_f} \dot{M}_L h_L \, dt + \int_{t_i}^{t_f} \dot{Q} \, dt \tag{21}$$

Rearranging terms gives

$$\int_{t_i}^{t_f} \underbrace{\left(\dot{M}_G h_G + \dot{Q}\right) dt}_{\text{Total energy added } (\Delta U_T)} = \int_{t_i}^{t_f} \underbrace{\left(\dot{M}_L h_L \, dt + dU_L\right)}_{\text{Total change in liquid in tank + liquid expelled energy } (\Delta U_L)} + \int_{t_i}^{t_f} dU_u + \int_{t_i}^{t_f} dU_w \tag{22}$$

Total change in ullage energy (ΔU_U)

Total change in wall energy (ΔU_W)

and dividing through by ΔU_T gives

$$1 = \frac{\Delta U_L}{\Delta U_T} + \frac{\Delta U_U}{\Delta U_T} + \frac{\Delta U_W}{\Delta U_T} \tag{23}$$

The data presented herein are in the form of these ratios. These ratios show the relative distribution of the total energy input.

TABLE I. - EXPERIMENTAL AND ANALYTICAL MASS BALANCE RESULTS

Run	Injector	Tank pressure, N/m^2	Volume discharge, m^3	Inlet gas temperature, K	Ramp time, sec	Hold time, sec	Expulsion time, sec	Tank cycle time, sec	Ramp period			Hold period				Expulsion period				
									Initial ullage mass, kg	Mass added during ramp, kg	Mass transfer during ramp, kg	Ullage mass after ramp, kg	Mass added during hold, kg	Mass transfer during hold, kg	Ullage mass after hold, kg	Mass added during expulsion, kg	Mass transfer during expulsion, kg	Final ullage mass, kg	Mass added during expulsion, kg (a)	Mass transfer during expulsion, kg (a)
14	Hemisphere	34.7×10^4	1.50	271	15.0	20.9	261.3	297.2	0.167	0.049	0.029	0.188	0.042	0.025	0.205±0.002	1.369±0.001	-0.248±0.119	1.822±0.058	1.308	-0.178
15		34.7	1.45	266	15.4	20.3	295.0	330.7	.224	.054	-.009	.287	.048	.021	.314±0.005	1.382±0.001	-.119±0.074	1.816±0.062	1.285	-.202
17		34.9	1.57	271	13.4	22.3	474.7	510.4	.079	.031	-.002	.112	.029	.006	.134±0.001	1.548±0.003	-.286±0.070	1.968±0.077	1.545	-.326
18		34.9	1.56	278	13.2	22.6	204.1	239.9	.103	.028	.008	.122	.021	-.001	.145±0.001	1.271±0.002	-.153±0.045	1.569±0.041	1.234	-.120
20		34.8	1.58	280	12.7	23.1	132.4	168.2	.053	.025	.009	.087	.014	-.010	.111±0.001	1.121±0.001	-.109±0.036	1.342±0.026	1.101	-.083
60		35.7	0	~333	32.0	158.5	-----	190.5	.063	.031	.004	.090	.022	-.228	.341±0.004	----------	----------	----------	-----	------
63		35.2	1.59		14.7	22.4	531.9	569.4	.061	.034	.027	.068	.027	.003	.092±0.001	1.565±0.002	-.355±0.091	2.012±0.082	1.538	-.382
64		34.7	1.59		14.2	22.8	377.6	414.7	.064	.022	.014	.071	.016	-.025	.112±0.001	1.410±0.001	-.255±0.067	1.777±0.063	1.359	-.248
65			1.58		14.3	22.6	354.5	391.4	.079	.019	.006	.093	.014	.009	.098±0.001	1.354±0.001	-.266±0.080	1.718±0.057	1.312	-.225
67			1.56		15.6	21.6	263.7	300.9	.089	.034	.023	.100	.029	.010	.120±0.001	1.285±0.001	-.218±0.076	1.623±0.049	1.212	-.191
68			1.58		15.0	22.1	149.0	186.1	.068	.026	.002	.092	.021	.012	.102±0.001	1.057±0.002	-.136±0.060	1.295±0.028	1.011	-.124
69		35.7	0	167	32.8	177.9	-----	210.7	.089	.039	.036	.093	.028	-.041	.161±0.002	----------	----------	----------	-----	------
70		34.7	0		29.4	150.1	-----	179.5	.073	.028	-.015	.116	.019	-.043	.176±0.002	----------	----------	----------	-----	------
71			1.58		14.3	23.6	406.3	442.2	.071	.039	.036	.077	.027	-.020	.123±0.001	1.705±0.003	-.235±0.086	2.063±0.081	1.679	-.324
73			1.57		13.8	24.1	288.9	326.8	.100	.035	.001	.135	.023	.014	.144±0.001	1.652±0.002	-.129±0.068	1.926±0.060	1.601	-.166
74			1.58		13.4	24.5	142.8	180.7	.061	.033	.0005	.093	.020	-.004	.116±0.001	1.426±0.001	.056±0.010	1.486±0.023	1.452	.061
75			0		31.0	190.9	-----	221.9	.066	.039	.007	.097	.023	-.046	.169±0.002	----------	----------	----------	-----	------
484	Radial	34.1×10^4	1.54	278	14.3	25.4	336.5	376.2	0.127	0.023	0.006	0.143	0.022	0	0.165±0.006	1.402±0.001	-0.274±0.037	1.841±0.070	1.372	-0.256
486			1.55	288	13.5	26.3	277.3	317.1	.127	.018	.012	.134	.013	-.026	.173±0.002	1.344±0.001	-.196±0.027	1.714±0.061	1.320	-.207
487			1.54	291	14.3	25.6	191.1	231.0	.133	.024	.005	.161	.019	.015	.166±0.006	1.221±0.001	-.150±0.033	1.536±0.040	1.191	-.146
488			1.54	293	14.5	25.1	134.8	173.9	.127	.024	.008	.143	.020	.001	.162±0.005	1.088±0.001	-.118±0.026	1.369±0.027	1.091	-.107
489			1.54	284	14.0	25.4	402.9	442.3	.120	.022	-.003	.145	.019	-.004	.167±0.007	1.435±0.002	-.302±0.067	1.904±0.078	1.422	-.303
490	Straight	34.3×10^4	1.55	290	15.4	24.4	402.5	442.3	0.121	0.028	0.021	0.128	0.021	-0.027	0.176±0.002	1.292±0.002	-0.329±0.033	1.798±0.059	1.279	-0.283
491	pipe		1.55	289	14.7	24.7	334.7	374.1	.114	.026	.007	.133	.019	.005	.147±0.002	1.226±0.002	-.349±0.047	1.722±0.068	1.231	-.231
492			1.54	289	14.7	24.7	275.5	314.9	.139	.024	.027	.137	.020	-.020	.176±0.002	1.156±0.001	-.234±0.026	1.566±0.045	1.149	-.185
493			1.54	289	14.7	24.8	190.3	229.8	.142	.027	.025	.143	.020	-.001	.164±0.002	1.014±0.001	-.223±0.019	1.400±0.031	1.054	-.126
494			1.55	291	14.8	24.6	135.6	175.0	.119	.026	.013	.133	.019	.005	.147±0.002	.895±0.001	-.187±0.014	1.229±0.022	.964	-.088
1	Hemisphere	34.2×10^4	1.51	294	23.2	29.3	394.0	446.5	0.112	0.033	0.027	0.114	0.007	-0.039	0.165±0.003	1.338±0.001	-0.196±0.049	1.700±0.064	1.256	-0.275
2		34.2	1.52	294	22.7	29.5	332.5	384.7	.092	.033	.014	.111	.013	-.015	.139±0.001	1.310±0.001	-.162±0.031	1.611±0.049	1.211	-.253
3		34.1	1.52	285	23.0	29.6	275.9	328.5	.094	.039	.019	.114	.015	0	.129±0.001	1.272±0.001	-.150±0.032	1.550±0.047	1.175	-.237
4		34.2	1.54	287	22.9	29.5	193.9	246.3	.078	.034	-.006	.117	.014	.014	.140±0.001	1.192±0.002	-.110±0.032	1.420±0.036	1.116	-.156
5		34.1	1.53	289	22.8	29.7	138.2	190.7	.082	.032	.015	.099	.012	.033	.144±0.001	1.065±0.001	-.068±0.018	1.279±0.025	1.066	-.093

[a]Values predicted by analytical program.

TABLE II. - EXPERIMENTAL AND ANALYTICAL ENERGY BALANCE RESULTS

Run	Injector	Inlet gas temperature, K	Expulsion time, sec	Expulsion period							
				Energy added by pressurant gas, J		Energy added by environment, J	Energy gained by tank wall, ΔU_w, J		Energy gained by ullage, ΔU_u	Energy gained by liquid, ΔU_L, J	
				Experimental	Analytical		Experimental	Analytical		Experimental	Analytical
14	Hemisphere	271	261.3	$530.2 \pm 0.4 \times 10^4$	506.3×10^4	19.1×10^4	268.6×10^4	263.7×10^4	$169.1 \pm 2.1 \times 10^4$	$109.0 \pm 19.7 \times 10^4$	72.8×10^4
15		266	295.0	529.8±0.5	492.2	21.6	274.6	266.9	159.9±1.9	91.0±22.6	85.9
17		271	474.7	599.5±1.1	598.3	34.8	313.5	326.8	182.8±2.3	107.7±26.6	138.6
18		278	204.1	501.8±0.6	486.7	14.9	234.9	249.0	163.6±1.9	78.7±17.2	57.8
20		280	132.4	445.9±0.4	437.9	9.7	189.0	202.8	156.6±1.7	73.1±13.7	39.0
63		333	531.9	688.7±0.8	676.3	38.9	413.9	481.4	189.7±2.4	123.8±15.3	162.8
64			377.6	685.5±0.6	660.1	27.7	409.5	443.4	178.0±2.3	125.0±13.2	114.8
65			354.5	689.0±0.6	667.0	26.0	402.3	443.4	175.2±2.1	123.0±12.6	107.6
67			263.7	623.6±0.4	588.1	19.3	378.1	372.4	168.5±2.1	122.1±10.7	80.4
68			149.0	544.0±0.9	520.1	10.9	251.3	290.8	156.5±1.8	109.6±15.5	45.4
71		167	406.3	449.4±0.7	442.2	29.8	194.6	181.2	186.9±2.4	111.4±12.7	123.3
73		167	288.9	413.7±0.4	400.9	21.2	162.2	143.0	178.2±2.2	80.5±11.2	88.3
74		167	142.8	347.0±0.3	353.2	10.5	108.2	101.4	159.8±1.7	90.7±14.9	43.3
484	Radial	278	336.5	$550.6 \pm 0.5 \times 10^4$	538.5×10^4	24.6×10^4	283.7×10^4	295.0×10^4	$172.1 \pm 2.2 \times 10^4$	$97.5 \pm 22.2 \times 10^4$	102.7×10^4
486		288	277.3	539.5±0.4	529.8	20.3	263.9	286.6	166.0±2.0	73.7±20.7	84.9
487		291	191.1	496.9±0.4	484.5	13.4	222.2	249.3	157.8±1.8	63.9±17.0	65.0
488		293	134.8	445.2±0.3	446.1	9.9	154.7	208.4	150.3±1.7	55.0±14.9	41.4
489		284	402.9	569.3±0.6	563.6	29.5	309.9	316.6	174.9±2.3	104.7±24.4	122.5
490	Straight	290	402.5	$521.6 \pm 0.4 \times 10^4$	515.9×10^4	29.5×10^4	257.0×10^4	297.1×10^4	$169.9 \pm 2.1 \times 10^4$	$77.8 \pm 24.7 \times 10^4$	122.0×10^4
491	pipe	289	334.7	494.2±0.6	496.2	24.5	233.6	271.3	167.2±2.2	69.6±22.4	101.8
492		289	275.5	485.1±0.6	481.7	20.2	210.5	251.5	158.7±1.7	73.3±20.2	83.7
493		289	190.3	410.5±0.5	426.5	13.9	168.1	208.7	151.3±1.5	54.4±17.2	57.9
494		291	135.6	365.3±0.3	393.4	9.9	130.4	178.4	145.2±1.6	48.3±14.8	41.3
1	Hemisphere	294	394.0	$546.7 \pm 1.5 \times 10^4$	512.8×10^4	28.8×10^4	294.8×10^4	269.1×10^4	$169.9 \pm 2.2 \times 10^4$	$76.1 \pm 24.4 \times 10^4$	126.5×10^4
2		294	332.5	529.5±1.4	489.3	24.3	273.6	247.5	167.7±2.0	80.4±22.2	105.5
3		285	275.9	514.0±2.1	474.4	20.2	251.8	231.5	165.7±2.0	85.4±20.2	87.9
4		287	193.9	484.1±0.8	453.1	14.2	225.8	205.2	160.6±1.9	83.0±17.2	62.3
5		289	138.2	434.4±5.5	434.4	10.1	197.6	171.4	152.1±1.7	65.6±14.9	44.5

Error Analysis

An analysis was performed to determine the magnitude of probable error which could be present in the integrations of equations (4) to (6) and in the determination of all terms in the energy balance equation (13). Probable error is defined as follows: There is a 50-percent probability that the error will be no larger than the value stated. This analysis considered the errors introduced by the inaccuracies of temperature transducers as well as the tank pressure sensor. These calculations were performed for all runs for the expulsion period. The results of this analysis are included with the tabular data in tables I and II.

RESULTS AND DISCUSSION

The main criterion used to compare the effectiveness of the various operating parameters on the amount of pressurant gas used is the nondimensional ratio M_I/M_G, where M_I is the ideal pressurant mass required to expel a given volume of liquid at a given inlet gas temperature and tank pressure. The actual pressurant requirement for the same conditions is M_G. A higher M_I/M_G ratio means less energy and mass exchange. It does not necessarily mean a lower absolute pressurant requirement M_G as will be illustrated later in this section.

For no environmental heating, a value of M_I/M_G equal to unity implies that no heat or mass transfer occurs. Therefore, from equation (23), the $\Delta U_U/\Delta U_T$ ratio is also equal to unity; that is, all the energy (ΔU_T) added to the tank during expulsion appears as an increase in ullage energy (ΔU_U). Accordingly, any value of M_I/M_G or $\Delta U_U/\Delta U_T$ less than unity means energy is lost by the ullage system. This loss of ullage energy would then appear as an increase in tank wall heating and/or liquid heating $\Delta U_W/\Delta U_T$ and $\Delta U_L/\Delta U_T$.

The discussion of results will first present the effects of the various operating parameters on the M_I/M_G ratio, for the expulsion period only, which was of primary interest, followed by the mass transfer M_t/M_G results. Then the results of the energy balances will be presented in an attempt to point out the major reason for the M_I/M_G or $\Delta U_U/\Delta U_T$ ratio being less than one. Finally a comparison will be made between the experimental results and the analytically predicted results to determine the validity of the analytical program. The analytical results are presented in the figures along with the corresponding experimental results. The comparison between experimental and analytical results will be given in terms of an average deviation. Average deviation is defined as

TABLE III. - DEVIATIONS BETWEEN EXPERIMENTAL ANALYTICAL RESULTS

Run	Injector	Inlet gas temperature, K	Tank wall thickness, cm	Percent deviation between experimental and analytical results[a]			
				M_I/M_G	M_I/M_{GN}	$\Delta U_W/\Delta U_T$	$\Delta U_L/\Delta U_T$
14	Hemisphere	271	0.762	+8.09	-8.50	+1.84	+28.6
15	↓	266	↓	+7.18	-.90	+3.01	+1.27
17		271		+10.45	-6.20	-4.25	-28.80
18		278		+6.33	-4.90	-6.37	+20.40
20		280		+5.86	-4.00	-8.00	+46.60
				Av +7.58	Av -4.90	Av 4.70	Av 25.13
63	Hemisphere	~333	0.762	+18.69	0	-16.16	-30.60
64	↓	↓	↓	+12.45	-3.50	-8.04	+2.86
65				+11.97	-5.50	-8.06	+9.88
67				+8.36	-7.00	+1.36	-33.70
68				+6.86	-5.30	-15.66	+57.10
				Av +11.67	Av -4.30	Av 9.86	Av 26.83
71	Hemisphere	167	0.762	+21.28	+10.60	+6.90	-9.92
73	↓	↓	↓	+18.02	+11.60	+11.80	-10.80
74				+16.69	+21.00	+6.27	+52.40
				Av +18.66	Av +14.40	Av 8.32	Av 24.4
484	Radial	278	0.762	+13.67	-2.90	-3.85	-5.31
486	↓	288	↓	+11.78	-1.00	-8.03	-16.03
487		291		+8.86	-2.50	-12.41	-1.60
488		293		+9.20	-.60	-11.19	-+1.80
489		284		+16.68	-.40	-2.32	-17.14
				Av +12.04	Av -1.50	Av 7.56	Av 12.98
490	Straight	290	0.762	+22.20	+3.62	-28.53	-58.90
491	pipe	289		+21.30	-1.05	-19.69	-23.90
492	↓	289	↓	+20.30	+4.37	-19.42	-10.00
493		289		+20.50	+3.62	-10.88	-8.60
494		291		+21.50	+5.16	-7.93	+13.95
				Av +21.16	Av +3.56	Av. 17.29	Av 23.07
1	Hemisphere	294	0.409	+11.56	0	+9.00	-66.70
2	↓	294	↓	+10.19	-1.00	+9.52	-31.70
3		285		+9.89	-.90	+8.07	-2.50
4		287		+6.44	-2.30	+9.28	+25.15
5		289		+8.06	-2.20	+13.06	+32.40
				Av +9.23	Av -1.30	Av 9.78	Av 31.69

[a]Analysis underpredicted, +; analysis overpredicted, -.

$$\left[\frac{\sum_{N}\left|\left(\begin{matrix}\text{Experimental}\\ \text{ratio}\end{matrix}\right)-\left(\begin{matrix}\text{Analytical}\\ \text{ratio}\end{matrix}\right)\right|}{\left(\begin{matrix}\text{Experimental}\\ \text{ratio}\end{matrix}\right)}\right](100) \qquad (24)$$

where N is the number of data points in a given set of operating conditions (i.e., when using a hemisphere injector for a constant inlet gas temperature of 167 K (301° R), N would be 3 for the data presented in fig. 8). For convenience, all deviations between the experimental and analytical results are summarized in table III.

The operating parameters (e.g., inlet gas temperature, injector geometry, tank wall thickness) and the major experimental and analytical results are summarized in tables I and II. Table I gives experimental and analytical mass balance results, while table II gives the corresponding energy balance results.

Temperature effect on pressurant gas requirements using a diffusing injector (hemisphere). - The effect of inlet gas temperature is shown in figure 8 on the basis of M_I/M_G for various expulsion times. Expulsion time is the total time required to expel liquid from a 5-percent ullage to a 95-percent ullage. Therefore, each data point represents a complete expulsion. As may be seen in the figure, the M_I/M_G ratio decreases for increasing inlet gas temperature. This implies a larger percentage of energy that is contained in the pressurant gas is lost to the tank wall and liquid as the inlet gas temperature is increased. The average decrease in M_I/M_G for all expulsion times in going from a 167 K (301° R) inlet gas temperature to a 273 K (491° R) inlet temperature is 27.0 percent.

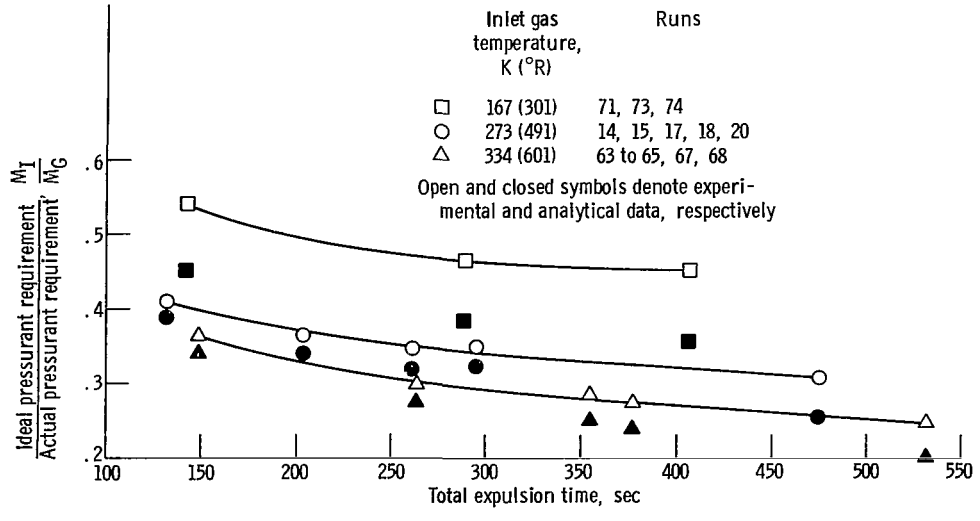

Figure 8. - Comparison of ideal pressurant requirement to actual pressurant requirement ratio as function of expulsion time for three inlet gas temperatures. Hemisphere injector; wall thickness, 0.762 centimeter (0.30 in.); tank pressure, 34.47×10^4 newtons per square meter (50 psia). Curves faired through experimental data.

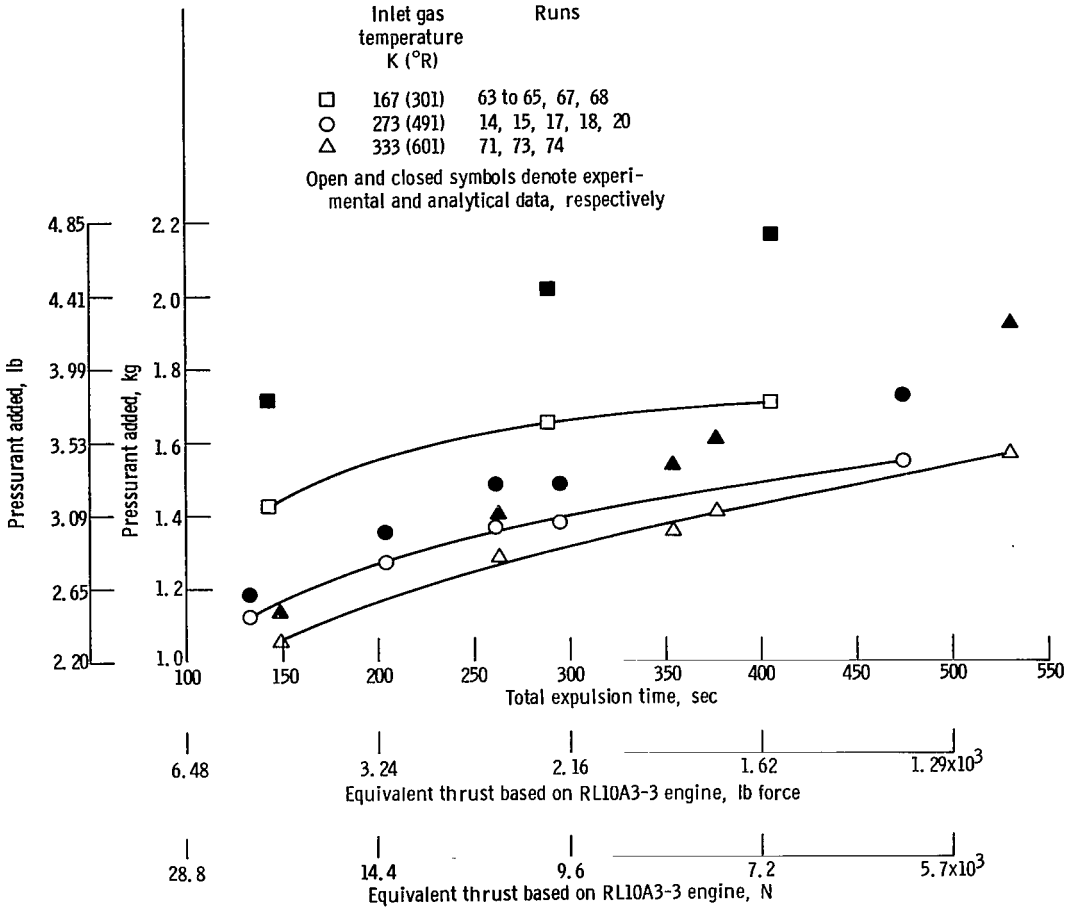

Figure 9. - Comparison of actual pressurant requirements for various expulsion times for three inlet gas temperatures. Hemisphere injector; tank wall thickness, 0.762 centimeter (0.30 in.); tank pressure, 34.47×10^4 newtons per square meter (50 psia). Curves faired through experimental data.

A comparison of the actual pressurant requirements M_G for the three inlet gas temperatures for various expulsion times is shown in figure 9. For convenience, the various expulsion times (or constant liquid outflow rates) are also shown in terms of an equivalent thrust level based on the specific impulse of the RL10A3-3 engine (I_S = 444 sec). The actual pressurant requirement M_G decrease for increasing inlet gas temperature and increase for increasing expulsion times. The data show an average reduction of 1.40 percent in pressurant gas requirements for a 10 K (18° R) increase in inlet gas temperature over the range of expulsion times. Although the absolute value of M_G decreases for increasing inlet gas temperatures, the M_I/M_G ratio also decreases because of the even greater decrease in ideal requirements. The average decrease in M_I/M_G in going from a 273 to 334 K (491° to 601° R) inlet gas temperature is 17.20 percent. For a given inlet gas temperature, there is an increasing pressurant requirement (decreasing M_I/M_G) for increasing expulsion times. The longer the pressurant (ullage) gas is exposed to cold surroundings, the greater the loss in pressurant energy.

The shaded symbols shown in figures 8 and 9 are the results as predicted by the

analytical program. The analysis underpredicts the ratio M_I/M_G, overpredicts the actual pressurant requirements, by an average of 12.64 percent for the three inlet gas temperatures (see table III, column (a), for actual deviations). The scatter of the analytical results is due to variations in the actual initial conditions (i.e., initial ullage volume, initial gas and wall temperatures, inlet gas temperatures, and pressure) that are used as input to the analytical program.

It should be kept in mind that this modified analysis still neglects mass transfer. Therefore all the predicted pressurant requirements must be supplied from a source external to the system (through the inlet injector), whereas in the true physical case (as will be shown later) some of the mass added to the ullage is supplied by the evaporation of liquid. At best the analytically predicted pressurant requirement should be greater than the experimental value by an amount equal to the mass evaporated (or less than the experimental value by an amount equal to the mass condensed).

If the comparison just presented were based on the net experimental mass added to the ullage M_{GN} (i.e., actual pressurant through injector plus any mass evaporated), the analysis overpredicts the M_I/M_{GN} ratio by an average of 4.60 percent for the 273 and 334 K (491° and 601° R) inlet temperatures and underpredicts the M_I/M_{GN} ratio by an average of 14.40 percent for the 167 K (301° R) inlet gas temperature (see table III, column (b)).

Because of this limitation imposed on the pressurant requirements as predicted by the analysis, the discussion of the comparisons between experimental and analytical pressurant requirements will include results based on both the actual pressurant added through the injector M_G and the net mass added to the ullage M_{GN}. The later comparison will do more justice to the analytical program and its assumptions.

A comparison of the ratio M_t/M_G of mass transferred during expulsion to the actual pressurant added to the tank is presented in figure 10 for different expulsion times and the three inlet gas temperatures. In all but one run, the net mass transfer was evaporation and represented between 8 and 23 percent of the pressurant mass added to the tank during expulsion. For two of the three inlet gas temperatures, the M_t/M_G ratio increases for increasing expulsion time. The same trend is present for the 167 K (301° R) temperature for expulsion times greater than 180 seconds. For a given expulsion time, the ratio increases for increasing inlet gas temperature.

The $\Delta U_U/\Delta U_T$ ratios of the energy increase in the ullage over the expulsion period to the total energy added to the tank is compared in figure 11 for different expulsion times and for the three inlet gas temperatures. For all runs, between 25 and 45 percent of the total energy that was added to the tank remains in the ullage after expulsion. For any given expulsion time, the $\Delta U_U/\Delta U_T$ ratio decreases (indicating increased energy loss to the wall and liquid) for increasing inlet gas temperatures. Also, for a given inlet gas temperature, the $\Delta U_U/\Delta U_T$ ratio decreases with increasing expulsion time. It should

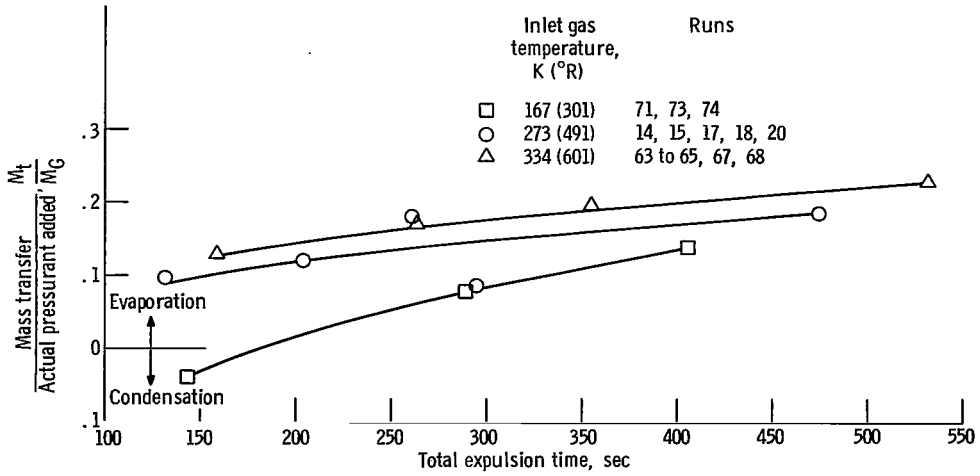

Figure 10. - Comparison of mass transfer to pressurant added ratio as function of expulsion time for three inlet gas temperatures. Hemisphere injector; tank wall thickness, 0.762 centimeter (0.30 in.); tank pressure, 34.47×10^4 newtons per square meter (50 psia). Curves faired through experimental data.

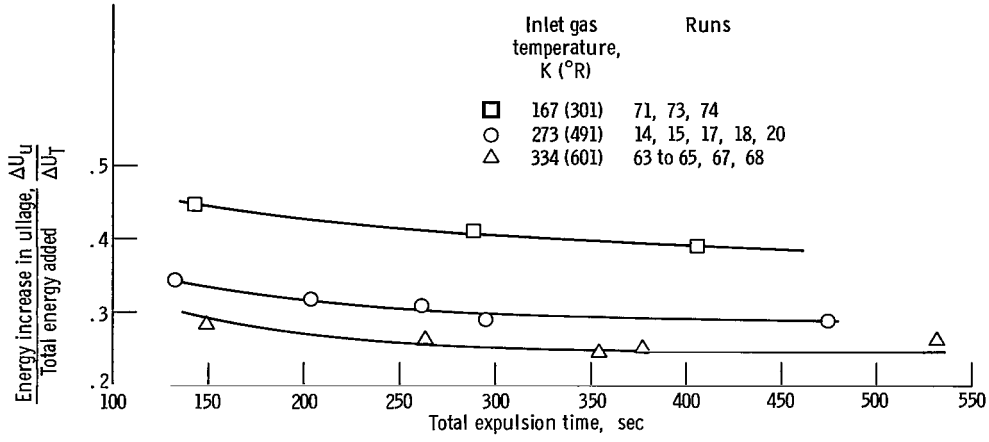

Figure 11. - Comparison of energy increase in ullage to total energy added ratio as function of expulsion time for three inlet gas temperatures. Hemisphere injector; tank wall thickness, 0.762 centimeter (0.30 in.); tank pressure, 34.47×10^4 newtons per square meter (50 psia).

be noted (table II) that the absolute value of ΔU_U does not change significantly for the various operating parameters used during testing. The two terms used in the determination of ΔU_U are ullage gas mass and specific internal energy. As the nominal value of inlet gas temperature is increased, the specific internal energy of the ullage gas necessarily is higher; however, the mass of gas in the ullage is significantly reduced. The net result of these two countering trends is to produce only a slightly decreasing value of ΔU_U for increasing inlet gas temperature. The mean increase in ullage energy for all runs was 166.2×10^4 joules (1576 Btu) with a standard deviation of 11×10^4 joules (104.5

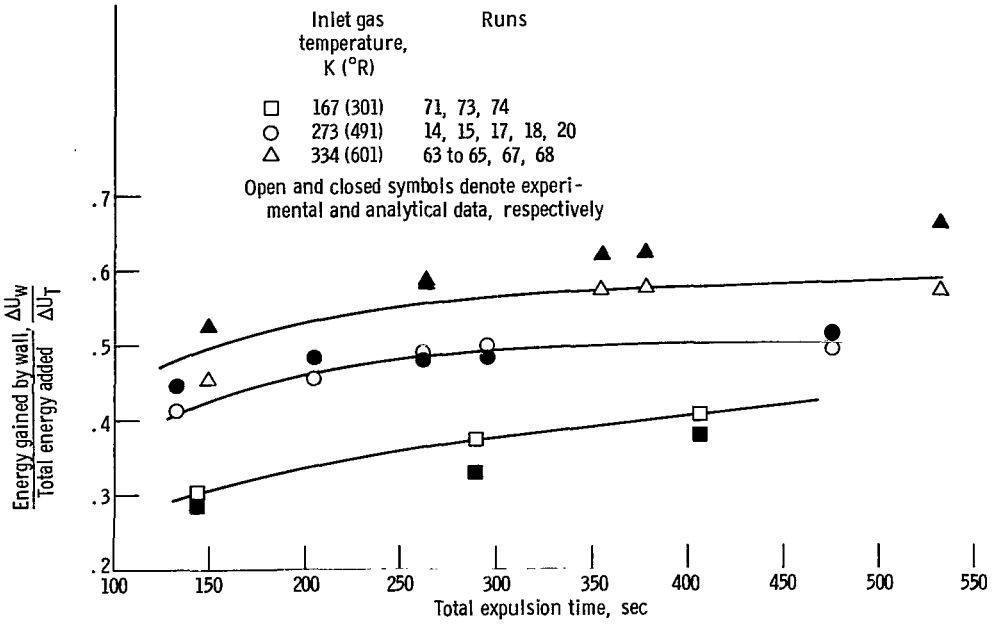

Figure 12. - Comparison of energy gained by wall to total energy added ratio as function of expulsion time for three inlet gas temperatures. Hemisphere injector; tank wall thickness, 0.762 centimeter (0.30 in.); tank pressure, 34.47×10^4 newtons per square meter (50 psia). Curves faired through experimental data.

Btu). Any trends in the $\Delta U_U/\Delta U_T$ ratio, therefore, depend mainly on variations in the total energy added (ΔU_T) to the tank due to variations in energy losses to the tank wall and liquid.

The ratio $\Delta U_W/\Delta U_T$ of energy gained by the tank wall to the total energy added is compared in figure 12 for three inlet gas temperatures for different expulsion times. In general, between 30 and 58.8 percent of the total energy added to the tank was gained by the tank wall over the range of conditions. As can be seen in table II and in figure 12, both the absolute value of ΔU_W and the $\Delta U_W/\Delta U_T$ ratio increase with increasing inlet gas temperature. The increase in ΔU_W is due to a larger driving potential (ΔT) for heat transfer between the ullage gas and the tank wall. The total energy added to the tank ΔU_T does not increase in the same proportion as ΔU_W, which results in the increasing $\Delta U_W/\Delta U_T$ ratio. Both the absolute value ΔU_W and the $\Delta U_W/\Delta U_T$ ratio also increase with increasing expulsion time. The increase in ΔU_W for increasing expulsion time is due to the longer exposure of the tank wall to a heat source.

Figure 13 is a comparison of the ratio of energy gained by the liquid to the total energy added to the tank $\Delta U_L/\Delta U_T$ for different expulsion times for the three inlet gas temperatures. In all cases, between 15 and 25 percent of the total energy added to the tank appears as an increase in energy of the liquid. There are no identifiable trends in the experimental data with either increasing inlet gas temperature or increasing expulsion time.

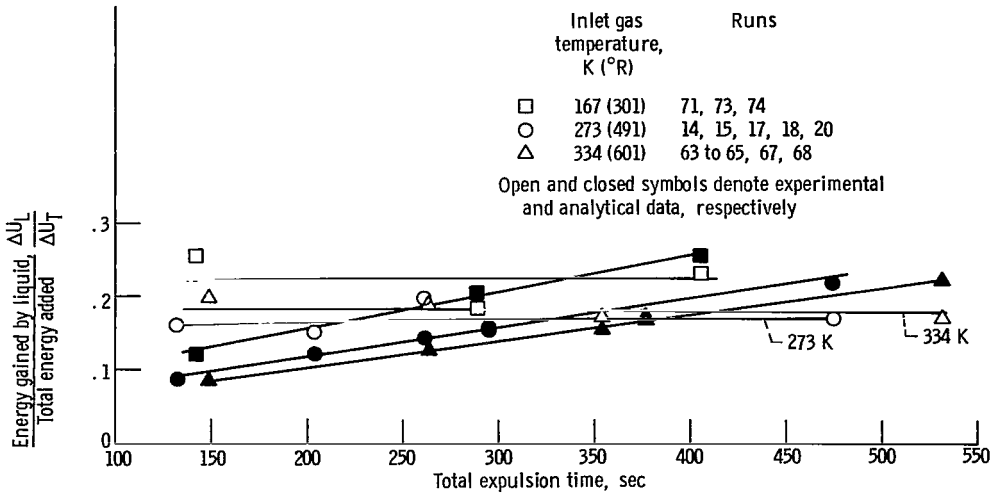

Figure 13. - Comparison of energy gained by liquid to total energy added ratio as function of expulsion time for three inlet gas temperatures. Hemisphere injector; tank wall thickness, 0.762 centimeter (0.30 in.); tank pressure, 34.47×10^4 newtons per square meter (50 psia).

The analytical predictions of the ratio $\Delta U_L/\Delta U_T$ are also presented in figure 13. (See table III for average deviations.) The large discrepancy between analysis and experiment could be the result of the error in experimentally determining ΔU_L. The probable error associated with each experimental determination of ΔU_L is between 8.8 and 25 percent (see table II). The analysis generally underpredicts the ratio below 340 to 380 second expulsion and overpredicts the ratio above 340 to 380 second expulsion. While the actual data showed no trends with either expulsion time or inlet gas temperature, the analysis does. The analysis predicts decreasing $\Delta U_L/\Delta U_T$ with increasing inlet gas temperature for constant expulsion time and predicts increasing $\Delta U_L/\Delta U_T$ with increasing expulsion time for constant inlet temperature.

The results from the preceding discussion point out that in all cases between 73.5 and 85 percent of the total energy that was added to the tank is either absorbed by the tank wall or remains in the ullage. The correlation between the analysis and experimental data, therefore, depends largely on the ability of the analysis to predict final wall and ullage gas temperature profiles. These temperature profiles are, in turn, used to determine the increase in wall and ullage energy and the final ullage mass. The ability to predict these temperatures explains the good agreement between experimental data and analysis reported in reference 1.

Figures 14 to 16 present comparisons of experimental and analytical wall and ullage gas temperature profiles. Three particular runs were selected to represent cases where (1) the agreement between analytical and experimental values of $\Delta U_W/\Delta U_T$ was the best, (2) the analysis overpredicts $\Delta U_W/\Delta U_T$, and (3) the analysis underpredicts $\Delta U_W/\Delta U_T$.

Figure 14 presents a comparison of experimental and analytical wall and ullage gas

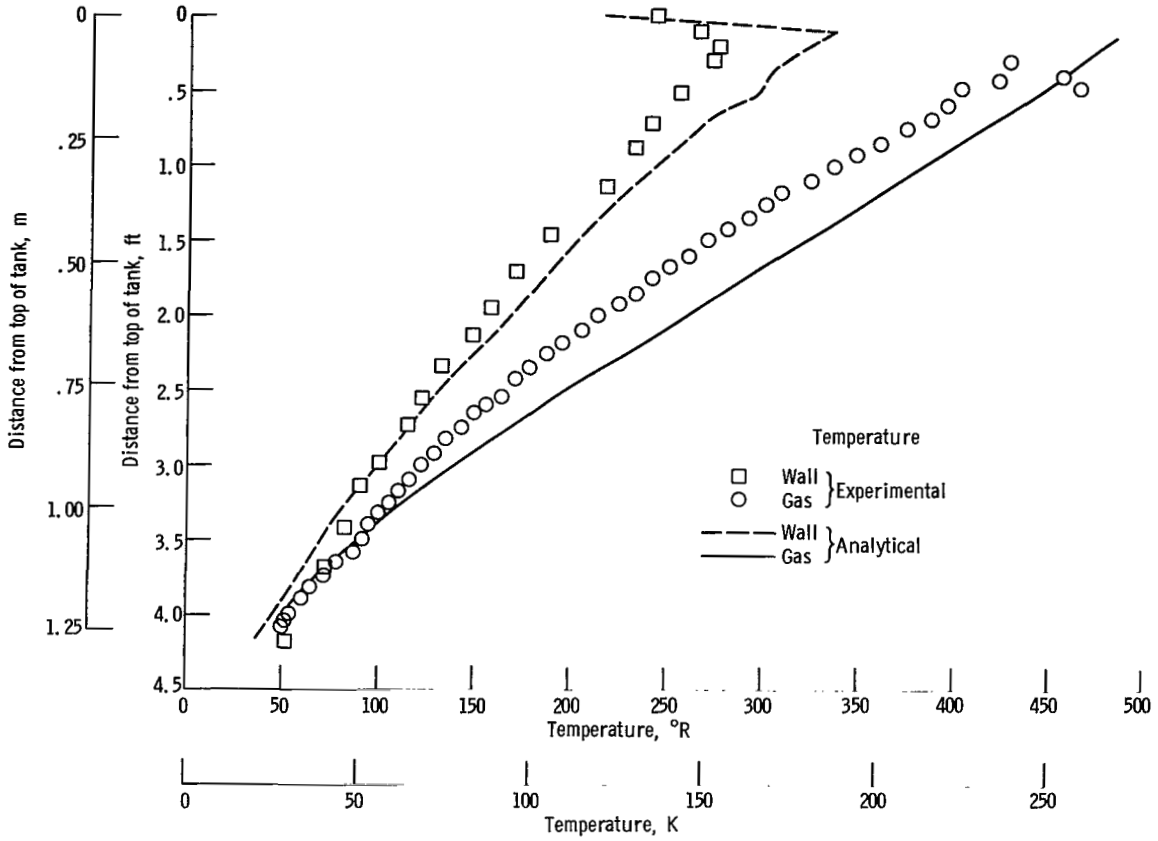

Figure 14. - Comparison of analytical and experimental gas and wall temperatures at end of 261-second expulsion. Hemisphere injector; inlet gas temperature, 271 K (488° R); tank wall thickness, 0.762 centimeter (0.30 in.); tank pressure, 34.47×10^4 newtons per square meter (50 psia); run 14.

temperature profiles for a run where the ratios M_I/M_G and $\Delta U_W/\Delta U_T$ that were predicted by the analysis were within 8.09 and 1.84 percent of the experimental results. The experimental gas temperatures shown on figure 14 are obtained from the vertical rake and indicate average radial temperatures at their respective vertical positions. In the absence of any mass transfer, the pressurant mass required for an expulsion could be determined as the difference between the final mass in the ullage and the initial mass prior to expulsion. Since one of the initial conditions for the analytical program is the initial experimental temperature profile (and, therefore, the initial ullage mass) prior to expulsion, the deviation in pressurant requirements would largely be the result of the predicted final temperature profile. As seen in figure 14, the calculated gas temperatures are slightly lower than the experimental temperatures in the lower 18 percent of the ullage (where 35 percent of the experimentally determined ullage mass is concentrated) but much higher in the remaining ullage. However, due to the temperature-density relation, the mass present in the final ullage volume for the two profiles differ by only 10 percent. The 10 percent deviation in final ullage mass plus the fact that the analysis

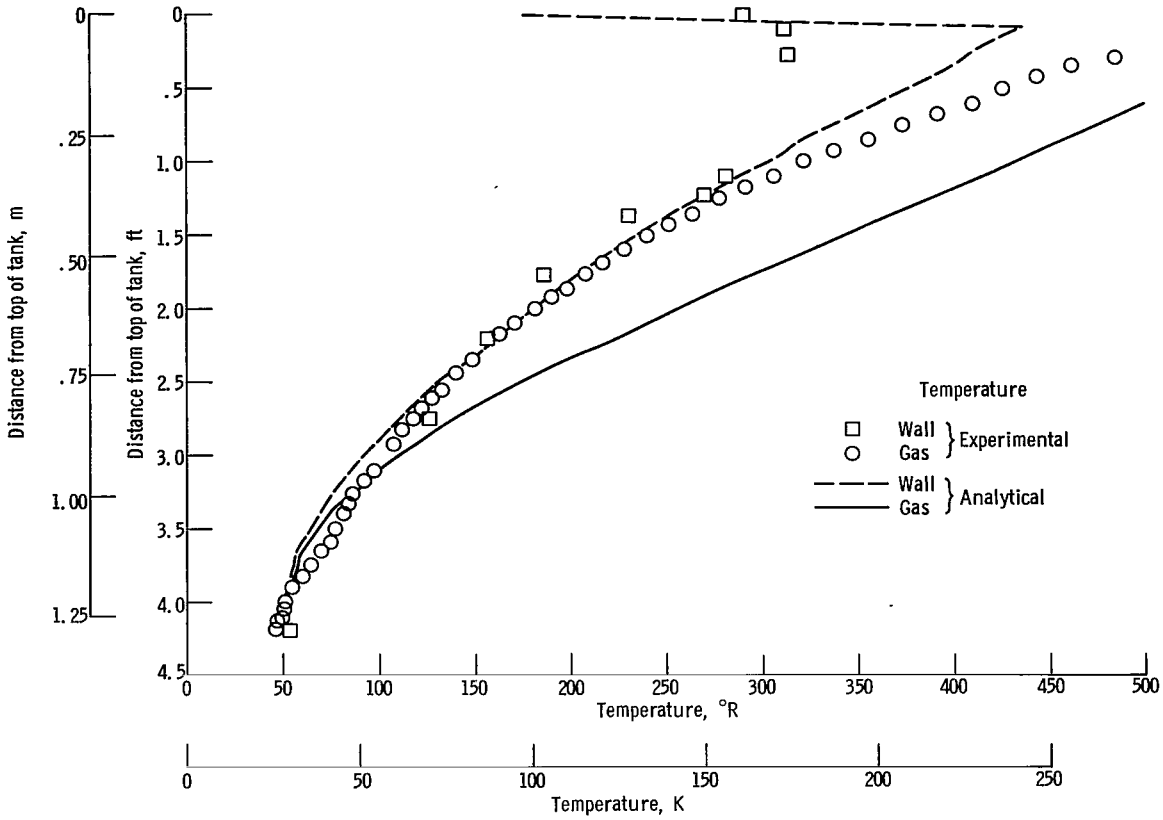

Figure 15. - Comparison of analytical and experimental gas and wall temperatures at end of 532-second expulsion. Hemisphere injector; inlet gas temperature of 334 K (601° R); tank wall thickness, 0.762 centimeter (0.30 in.); tank pressure, 34.47×10^4 newtons per square meter (50 psia); run 63.

neglects mass transfer account for the 8.09 percent deviation in M_I/M_G ratio (8.5 percent in M_I/M_{GN} ratio).

The analytically predicted wall temperatures (fig. 14) are very close to those observed experimentally in the lower half of the tank ullage but begin to get higher toward the top of the tank. Even though the analytical wall temperatures are higher in the upper portion of the tank wall, the analysis underpredicts ΔU_W by 1.84 percent. All values of energy gained by the tank wall (ΔU_W) include the energy gained by the tank lid. The tank lid is approximately 22 percent of the total tank mass. The final lid temperature, both predicted and actual are shown as the uppermost wall temperature (point zero in fig. 14). The predicted lid temperature is 15.5 K (28° R) lower than the observed temperature. The underprediction of temperature for a large mass concentration together with the fact that the specific heat of the wall is a strong function of temperature apparently offsets the increase in wall energy due to overpredicting the temperatures in the upper portion of the tank wall.

Figure 15 is a comparison of experimental and analytical wall and ullage gas temper-

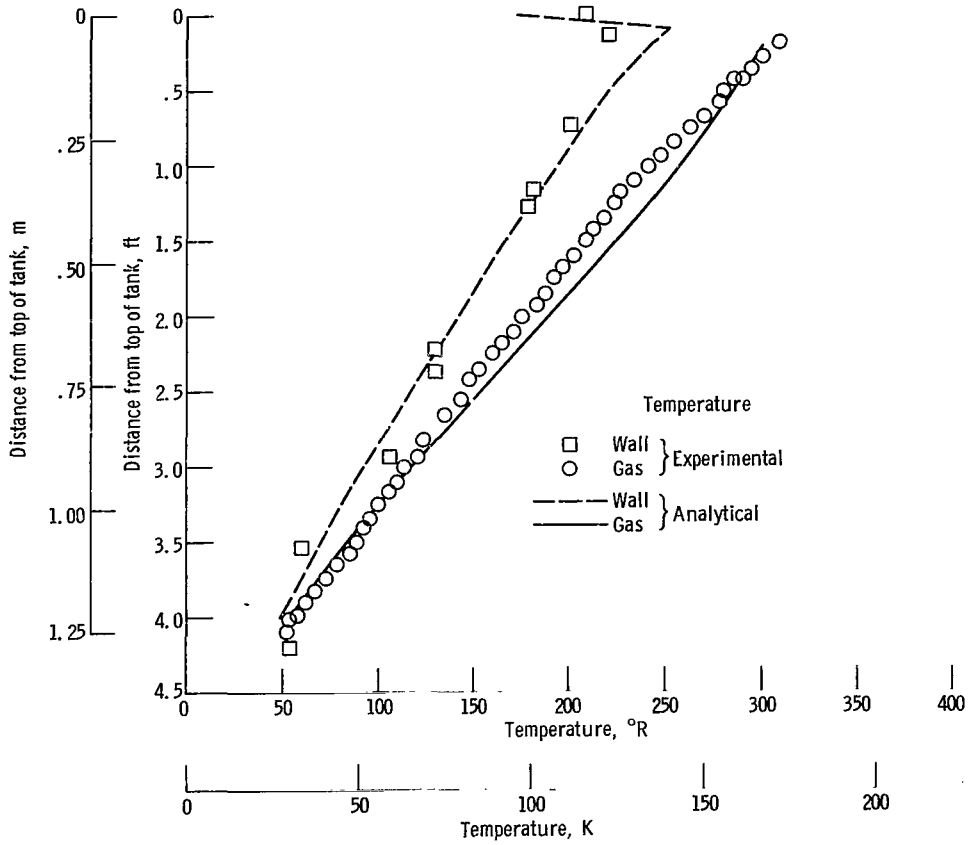

Figure 16. - Comparison of analytical and experimental gas and wall temperatures at end of 289-second expulsion. Hemisphere injector; inlet gas temperature, 167 K (301° R); tank wall thickness, 0.762 centimeter (0.30 in.); tank pressure, 34.47x10^4 newtons per meter (50 psia); run 73.

ature profiles for a run which had an inlet gas temperature of 334 K (601° R). Here again, the calculated ullage gas temperatures are lower than the experimental temperatures in the lower 25 percent of the ullage (where 46 percent of the ullage mass is concentrated) but much higher in the remaining ullage. The total final ullage mass is approximately the same for both profiles. As a result, the deviation between the analytical and experimental values of M_I/M_G is entirely due to the analysis neglecting mass transfer.

The analytically predicted wall temperatures agree fairly well with the experimental temperatures except in the upper 25 percent of the wall where the analysis overpredicts temperatures as much as 58 K (104° R). For this run, the analysis overpredicts the energy gained by the wall. In this case, the underprediction of lid temperature (point zero in fig. 15) does not offset the increase in wall energy due to the large overprediction of wall temperatures in the upper portion of the tank wall.

A comparison of experimental and analytical wall and ullage gas temperatures for a run which had an inlet gas temperature of approximately 167 K (301° R) is shown in figure 16. Here the analytical wall and gas temperatures are very close to those obtained

experimentally. However, the analytical prediction of the mass ratios M_I/M_G or M_I/M_{GN} was poor (typical of the 167 K (301° R) prediction). The analysis underpredicts the energy gained by the wall as a result of underpredicting the temperature rise of the lid.

From the preceding discussion it is evident that the analysis predicted accurately the pressurant requirements even though the analysis, in most cases, did not accurately predict the temperature profile in the ullage after the expulsion. The fair agreement between the analysis and observed requirements is because the "mass weighted average temperatures" $\left(\text{given by } \left(\sum_i^{V_U} M_i T_i\right) \Big/ M_{u,f}\right)$ is approximately equal for both the predicted and observed final temperature profiles.

Injector effect on pressurant requirements. - The effect of injector geometry on the M_I/M_G ratio for different expulsion times for an inlet gas temperature of 284±6.0 K (511±11° R) is shown in figure 17. The hemisphere and radial injectors (diffuser types) have approximately the same M_I/M_G ratio for the various expulsion times. The straight pipe, however, has lower pressurant requirements (a greater M_I/M_G ratio) than the diffuser-type injector for all expulsion times. The straight pipe injector required 20 percent less pressurant for a 135-second expulsion and 8.9 percent less for a 402-second expulsion. At some expulsion time greater than 500 seconds, the straight pipe and diffuser type injectors would appear to have the same pressurant requirement. At this point, the effect of the injection pattern of the straight pipe would be minimized due to the low injection velocities. It should be noted here that these are approximately the same results that were obtained in reference 3 with a small cylindrical tank. The reasons for the decreased pressurant requirements (increased M_I/M_G ratio) when using the straight pipe injector are (1) less heat transfer to the tank walls and (2) a greater evaporation of liquid. These two facts will be discussed further later in this section. All three injectors have increasing pressurant requirements (decreasing M_I/M_G ratio) for increasing expulsion times.

The analytical predictions for the three injectors can be approximated by a single curve as shown in figure 17. Since inlet gas temperature and tank pressure as functions of time and liquid flow rate are the only required inputs to the analytical program, it is not surprising that the M_I/M_G ratio is not a function of injector design. The analytical predictions of M_I/M_G are better for the diffuser type injectors because this type best approximates the one-dimensional flow assumption of the analysis. The average deviation between the analytical and experimental values of M_I/M_G for the diffuser type injectors is 9.81 percent compared to 21.16 percent for the straight pipe injector.

The agreement between analysis and experimental values of M_I/M_{GN} are good for all three injectors. The average deviation for all three injectors is 3.67 percent. The

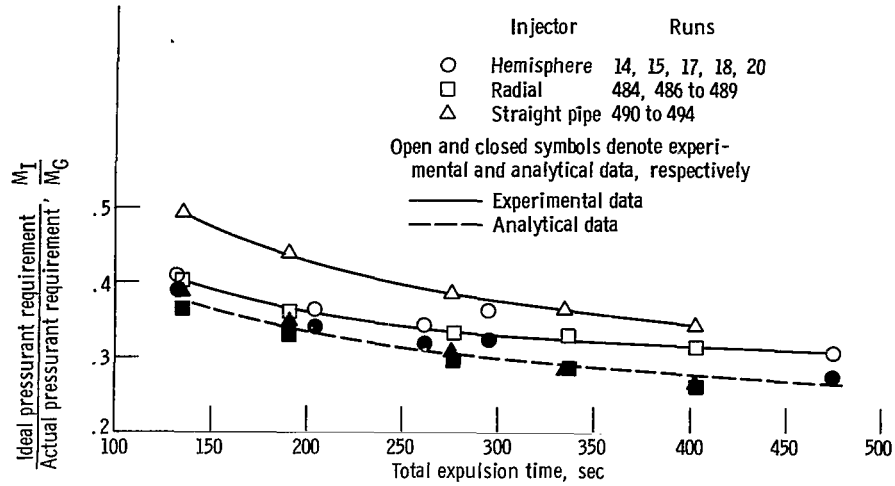

Figure 17. - Comparison of ideal pressurant requirement to actual pressurant requirement ratio as function of expulsion time for three injector geometries. Inlet gas temperature, 284±6 K (511°±11° R); tank wall thickness, 0.762 centimeter (0.30 in.); tank pressure, 34.47×10^4 newtons per square meter (50 psia).

improved agreement, especially for the straight pipe injector, is probably the result of compensating limitations or assumptions of the analytical program. This compensation will be discussed later in this section.

The comparison of the M_t/M_G ratios for different expulsion times for the three injector geometries is shown in figure 18. In general, all injectors show increased M_t/M_G (increased evaporation) with increasing expulsion time. The straight pipe injector has a higher M_t/M_G ratio (more evaporation) for all expulsion times than the diffuser type (93.5 percent higher than the radial injector at a 135-sec expulsion and 21.4

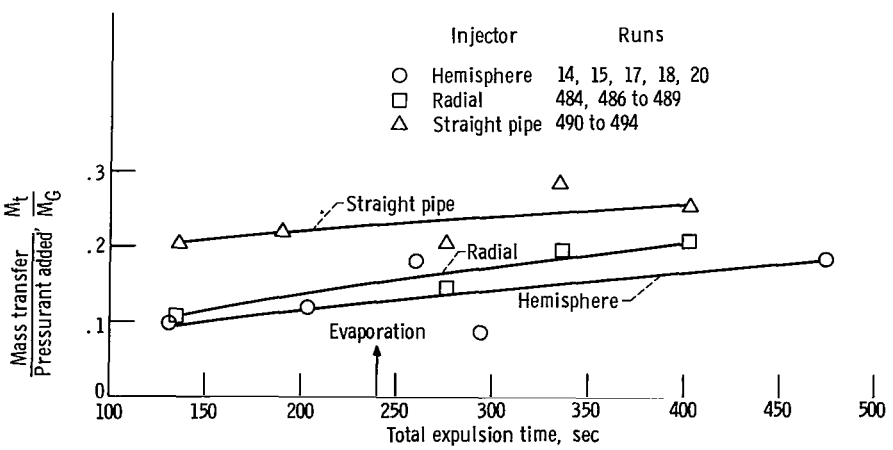

Figure 18. - Comparison of a mass transfer to pressurant added ratio as function of expulsion time for three injector geometries. Inlet gas temperature, 284±6 K (511°±11° R); tank wall thickness, 0.762 centimeter (0.30 in.); tank pressure, 34.47×10^4 newtons per square meter (50 psia).

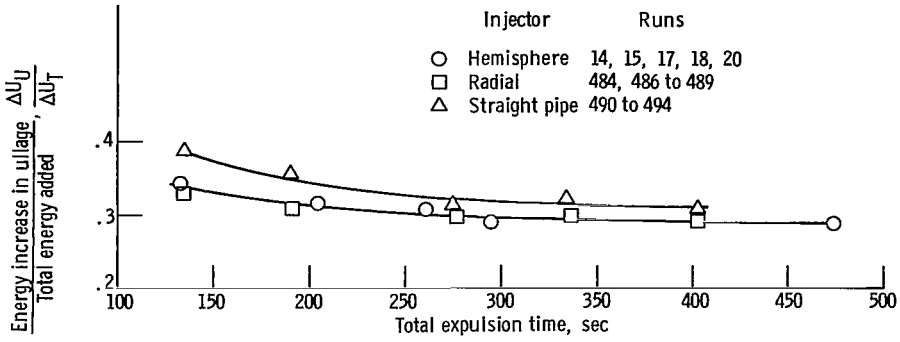

Figure 19. - Comparison of energy increase in ullage to total energy added ratio as function of expulsion time for three injector geometries. Inlet gas temperature 284±6.0 K (511°±11° R); tank wall thickness, 0.762 centimeter (0.30 in.); tank pressure, 34.47×10^4 newtons per square meter (50 psia).

percent higher at a 402-sec expulsion). Of the diffuser type injectors, the radial injector has the higher M_t/M_G (11.3 percent higher than the hemisphere at 135-sec expulsion and 23.5 percent higher at 402-sec expulsion).

The comparison of the $\Delta U_U/\Delta U_T$ ratio for different expulsion times for the three injector geometries is shown in figure 19. In general, $\Delta U_U/\Delta U_T$ decreases with increasing expulsion time for the three injector geometries. The diffuser type injectors (hemisphere and radial) have approximately the same $\Delta U_U/\Delta U_T$ ratio for the various expulsion times. Figure 19 indicates that, for the diffuser type injectors, between 29 and 34 percent of the total energy added to the tank remains in the ullage at the end of the expulsion periods. The straight pipe has an average 9.3 percent higher $\Delta U_U/\Delta U_T$ ratio than the diffuser type injectors. For the straight pipe, between 31.0 and 39.0 percent of the total energy added to the tank remains in the ullage after expulsion.

The ratio of energy gained by the tank wall to the total energy added to the 0.762

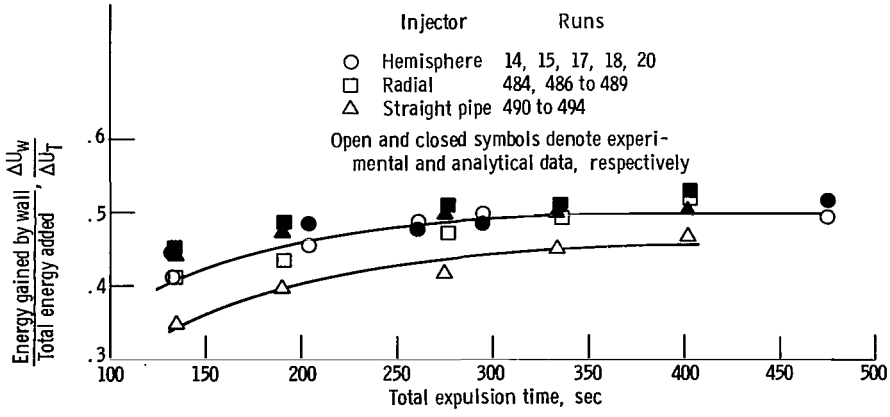

Figure 20. - Comparison of energy gained by wall to total energy added ratio as function of expulsion time for three injector geometries. Inlet gas temperature, 284±6 K (511°±11° R); tank wall thickness, 0.762 centimeter (0.30 in.); tank pressure, 34.47×10^4 newtons per square meter (50 psia). Curves faired through experimental data.

centimeter (0.30 in.) thick tank wall $\Delta U_W/\Delta U_T$ for different expulsion times for the three injector geometries is shown in figure 20. The two diffuser type injectors have approximately the same $\Delta U_W/\Delta U_T$ ratios for the various expulsion times. The data presented can be represented by a single curve. The straight pipe injector causes less wall heating and a lower $\Delta U_W/\Delta U_T$ ratio than the diffuser types - 15.60 percent lower at a 135-second expulsion and 9.90 percent lower at a 402-second expulsion. All three injectors have increasing wall heating and increasing $\Delta U_W/\Delta U_T$ for increasing expulsion times. The increased wall heating is because the wall is exposed to a heat source for a longer duration for the longer expulsion times. The reduced wall heating when using the straight pipe is due to lower, nearly constant, axial temperature gradients in the upper portion of the ullage together with rather large radial temperature gradients that were lowest near the tank wall and highest at the center of the tank.

In general, the analysis overpredicts $\Delta U_W/\Delta U_T$ (fig. 20). The average deviation between analytical and experimental values of $\Delta U_W/\Delta U_T$ is 6.13 percent for the diffuser type injectors compared to 17.29 percent for the straight pipe injector. One of the assumptions made in the analytical program is that no radial temperature gradients exist in the ullage. This assumption is approximately true during expulsion with the diffuser type injectors (resulting in a fair analytical prediction of wall heating) but not true when using the straight pipe injector. Figure 21 compares the actual radial temperature profiles and the predicted ones while using the straight pipe injector.

Figure 22 presents a comparison of the $\Delta U_L/\Delta U_T$ ratio for different expulsion times for the three injector geometries. In all cases, between 12 and 20 percent of the total energy added to the tank appears as an increase in liquid energy. The data show no significant trend in $\Delta U_L/\Delta U_T$ with expulsion for any of the injector geometries. The probable errors associated with experimentally determining ΔU_L (see table II) are large enough to discourage any quantitative discussion. The straight pipe injector indicates less liquid heating (ΔU_L, table II) than the diffuser type injectors.

The decrease liquid heating and the increased evaporation obtained when using the straight pipe injector may be due to the inability of the liquid hydrogen to conduct heat from the surface to the bulk fluid at a rate equal to that at which the gas is adding heat to the surface. As a result, a local area of liquid at the surface quickly reaches the saturation point and evaporates, carrying with it some of the liquid's energy. The decrease in liquid heating when using the straight pipe injector may not occur for all tank geometries and sizes.

The analytical data presented in figure 22 indicate an increase in liquid heating (increasing $\Delta U_I/\Delta U_T$) for increasing expulsion times for all injectors. There is no appreciable variation in the predicted values of $\Delta U_L/\Delta U_T$ for the three injectors at the various expulsion times. What little scatter there is is due to variations in initial conditions

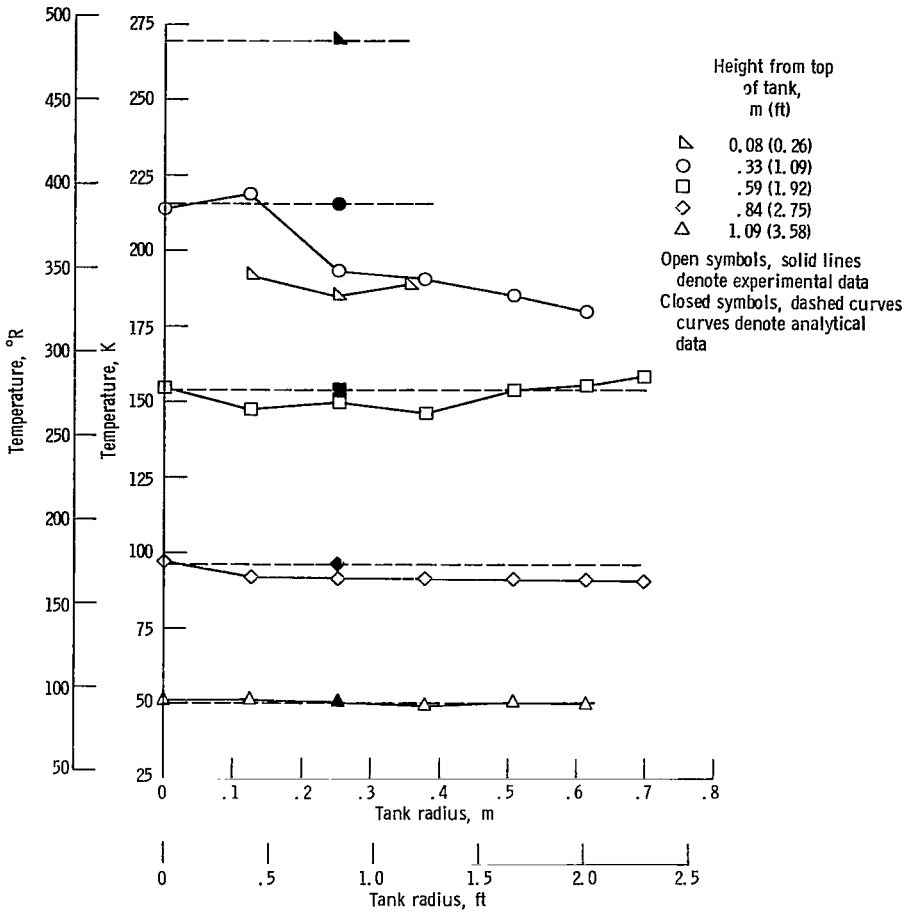

Figure 21. - Comparison of experimental and analytic radial gas temperatures at various axial positions in the tank at end of 276-second expulsion. Straight pipe injector; inlet gas temperature, 289 K (520° R); tank wall thickness, 0.762 centimeter (0.30 in.).

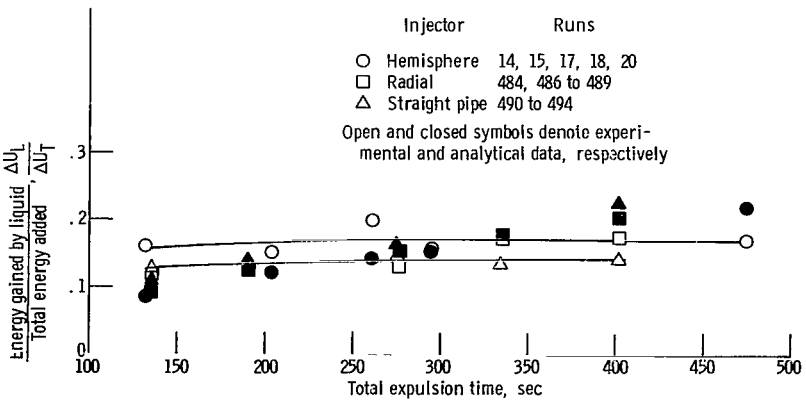

Figure 22. - Comparison of energy gained by liquid to total energy added ratio as function of expulsion time for three injector geometries. Inlet gas temperature, 284±6 K (511°±11° R); tank wall thickness, 0.762 centimeter (0.30 in.); tank pressure, 34.47×10^4 newtons per square meter (50 psia). Curves faired through experimental data.

(e.g., initial wall and gas temperature profiles, inlet gas temperature, and pressure) for the different injectors.

The amount of usable propellant is an important parameter when considering the overall optimization of a pressurization system. For a pressure-fed system, all the propellant would be usable. However, for a pump-fed system, the amount of usable propellant would depend on the temperature stratification buildup in the liquid and the net positive suctionhead (NPSH) of the pump. For a given outflow rate (expulsion time), the final temperature profile in the liquid was approximately the same for the various inlet gas temperatures and injector geometries used in this report. This means that for a given NPSH, the usable propellant would be the same regardless of inlet gas temperature or injector geometry. This result may not be true for different tank sizes or geometries or for different external heating rates.

Figures 23 and 24 compare experimental and calculated ullage gas and wall temperature profiles for a diffuser type injector (radial) and the straight pipe injector at the end of approximately a 276-second expulsion.

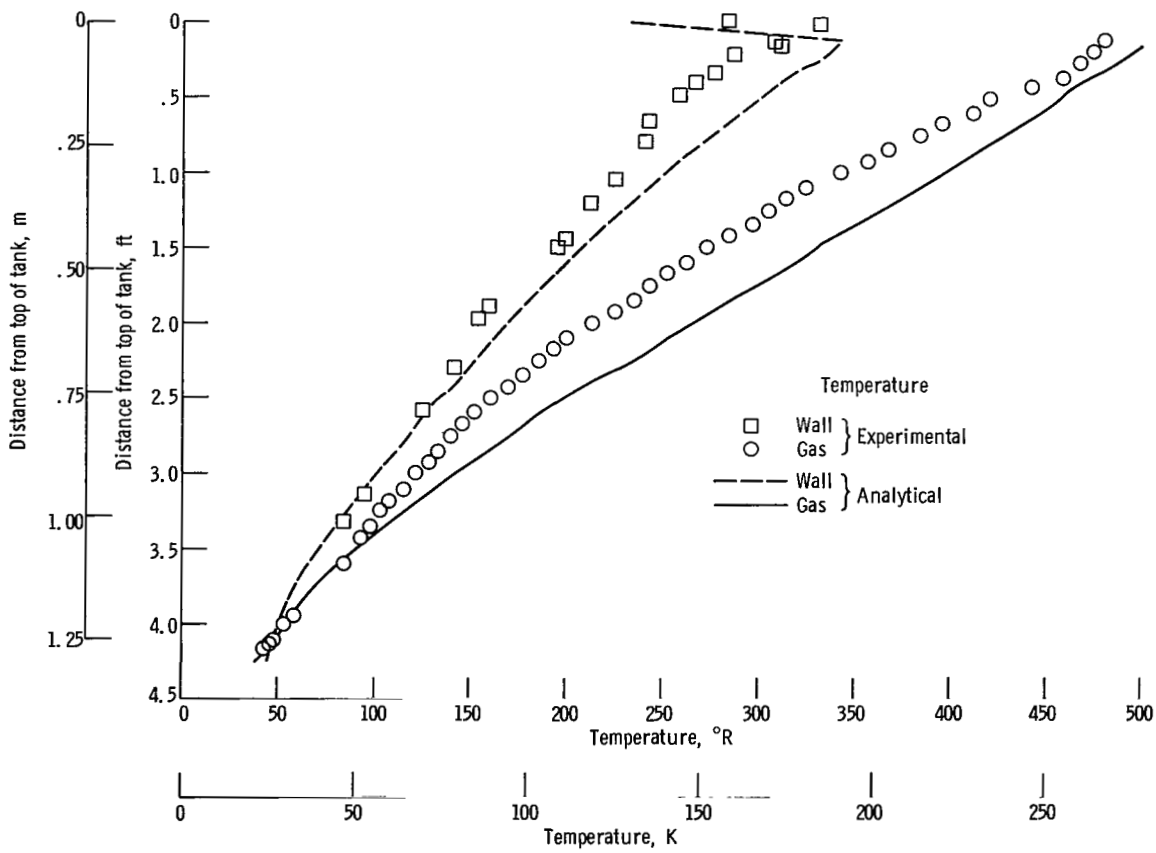

Figure 23. - Comparison of analytical and experimental gas and wall temperatures at the end of 277-second expulsion. Radial injector; inlet gas temperature, 288 K (518° R); tank wall thickness, 0.762 centimeter (0.30 in.); run 486.

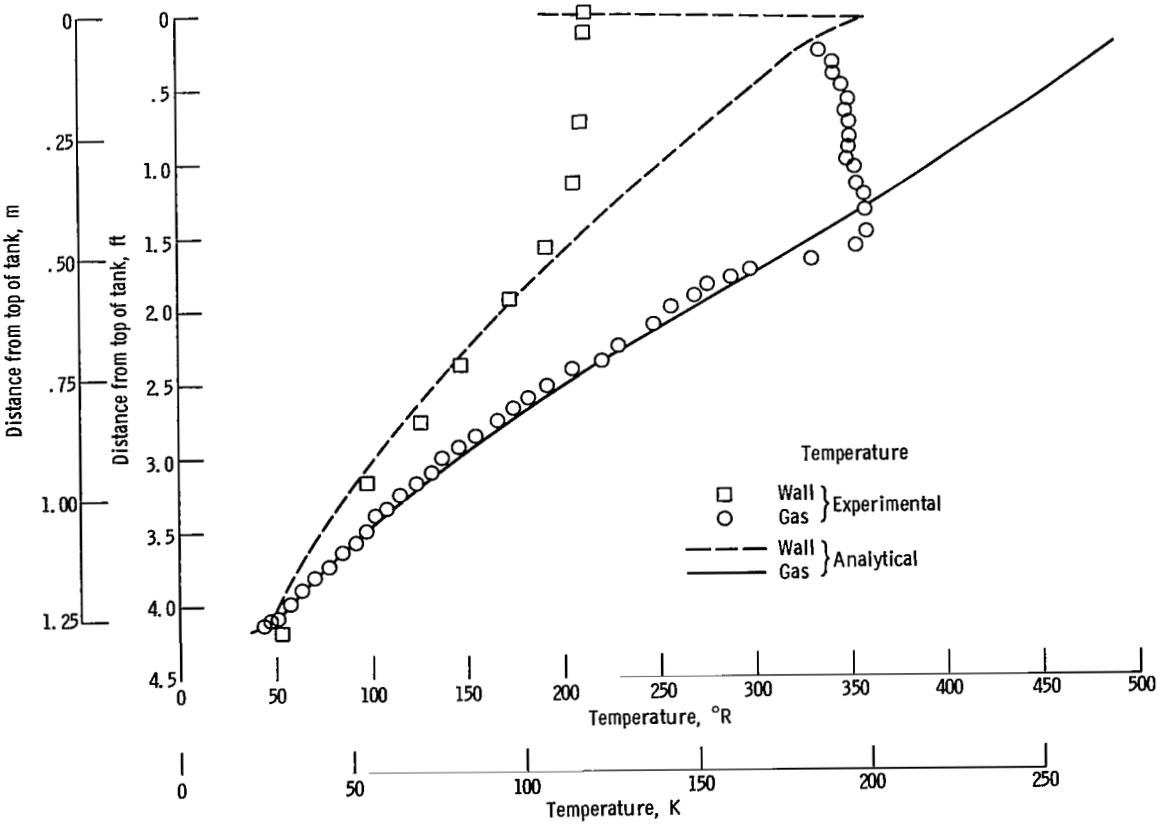

Figure 24. - Comparison of analytical and experimental gas and wall temperatures at end of 276-second expulsion. Straight pipe injector; inlet gas temperature, 289 K (520° R); tank wall thickness, 0.762 centimeter (0.30 in.); run 492.

The analysis overpredicts the tank wall temperatures (fig. 23) for the upper half of the tank wall when using the radial injector. The temperature overprediction accounts for the overprediction of 8.03 percent on $\Delta U_W/\Delta U_T$ (fig. 20). The analysis also overpredicts the ullage gas temperatures in the upper 70 percent of the ullage. In spite of this overprediction of ullage temperature, the analysis predicts the M_I/M_G ratio to within 1.00 percent of that which was determined experimentally. This again is due to the ability of the analysis to predict the mass average temperature which was previously discussed.

Figure 24 shows the effect that the straight pipe injector has on the wall and ullage gas temperature profiles. The experimental data show a nearly constant ullage temperature profile in the upper 40 percent of the ullage. The temperature then decreases almost linearly to the liquid surface. The experimental wall temperature profile is similar to that of the ullage. The analytical gas temperatures increase almost linearly from the liquid surface to the top of the tank. There is good agreement between the analytical and experimental wall and gas temperature profiles in the lower 60 percent of the tank, but

the analysis overpredicts both gas and wall temperatures in the upper 40 percent of the tank. The predicted (constant radial temperatures) and experimental radial gas temperature profiles for the run data shown in figure 24 are compared in figure 21. The predicted gas temperatures near the tank wall are with one exception higher than the experimental data. Thus, the larger overprediction of wall temperatures in the upper 40 percent of the tank coupled with the fact that the specific heat of aluminum rapidly increases with increasing temperature leads to the overprediction of 19.42 percent on $\Delta U_W/\Delta U_T$. The good agreement between the analytic and experimental temperatures in the lower 60 percent of the ullage (where approximately 87 percent of the total ullage mass is concentrated) is the reason there is good agreement between the analytic and experimental mass ratios based on the net mass added experimentally (M_{GN}).

The experimental results, when using the straight pipe injector, indicate non-one-dimensional flow and substantial mass transfer, both of which are contrary to the analytical assumptions. The close agreement between analysis and experimental mass ratios (M_I/M_{GN}) apparently is the result of one faulty analytic assumption compensating for another. These results would not necessarily be expected for tanks of different size or geometry or under different operating conditions.

Moreover, the analysis does not predict the distribution of the energy losses (i.e., $\Delta U_W/\Delta U_T$ or $\Delta U_L/\Delta U_T$). It is generally concluded that the present analytical model is not strictly usable in its present form for the analysis of the straight pipe injector.

Effect of tank wall thickness on pressurant requirements. - The results of reference 3 indicated that between 77 and 93 percent of the total energy lost by the pressurant gas was lost to the tank wall. It was expected, therefore, that tank wall thickness would play an important roll in determining the pressurant requirements during the expulsion period. Additional tests were performed using a 1.52-meter- (5-ft-) diameter spherical tank similar to the one already discussed except that the tank wall was chem-milled down to an average thickness of 0.409 centimeter (0.161 in.). Although the chem-milling reduced the wall thickness by 46.3 percent, the total weight of the tank was reduced by only 29.5 percent due to the structural requirement of keeping the same thickness for the tank neck, lid, and girth support.

Figure 25 presents a comparison of the M_I/M_G ratio for different expulsion times for the two tank wall thicknesses (0.762 and 0.409 cm; 0.30 and 0.161 in.). Each tank used the hemisphere injector. The average inlet gas temperature for the 0.409 centimeter (0.161 in.) tank was 290 K (~520° R). The average inlet gas temperature for the 0.762 centimeter (0.30 in.) tank was 273 K (~490° R). The 0.409 centimeter (0.161 in.) thick tank has an average of 6.5 percent less pressurant requirement, higher M_I/M_G ratio, than the 0.762 centimeter (0.30 in.) thick tank for all expulsion times. In most cases, the analysis again overpredicts the pressurant requirements (underpredicts the M_I/M_G ratio). See table III for deviations between analytical and experimental results.

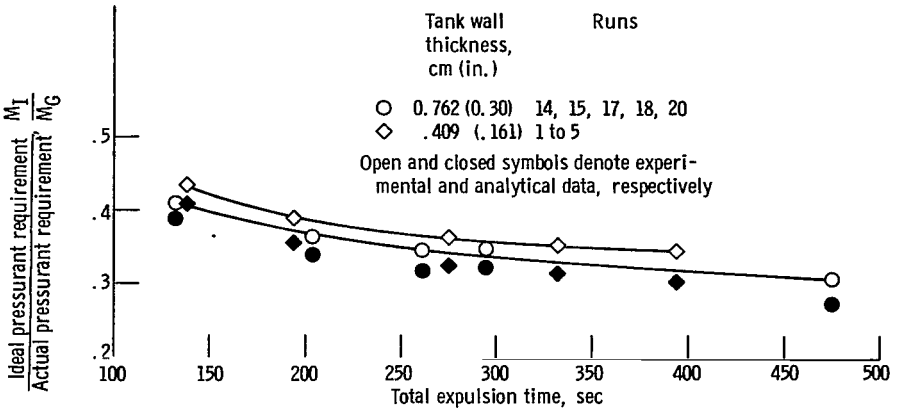

Figure 25. - Comparison of ideal pressurant requirement to actual pressurant requirement ratio as function of expulsion time for two wall thicknesses. Hemisphere injector; inlet gas temperature, 281±15 K (506°±27° R); tank pressure, 34.47x10^4 newtons per newtons per square meter (50 psia). Curves faired through experimental data.

The 6.5-percent decrease in pressurant requirements was less than expected. However, the test with the 0.409 centimeter (0.161 in.) thick tank had an average 17 K (31°R) higher inlet gas temperature. When based on the results already obtained on the effect of inlet gas temperature on pressurant requirements (fig. 8), this 17 K (31° R) higher inlet temperature would normally decrease the M_I/M_G ratio by approximately 4.8 percent. Thus, for equal inlet gas temperatures, a nominal decrease in pressurant requirements of approximately 11.0 percent would be expected for the 0.409 centimeter (0.161 in.) thick tank.

Figure 26 is a comparison of $\Delta U_W/\Delta U_T$ for different expulsion times for the two

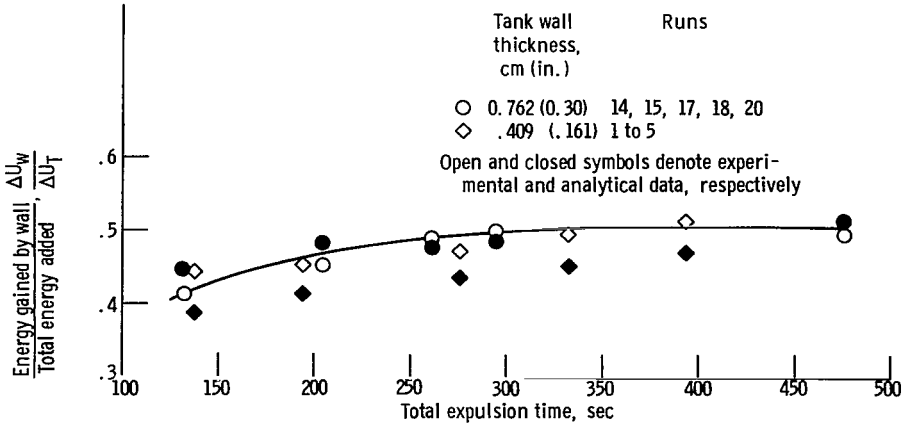

Figure 26. - Comparison of energy gained by wall to total energy added ratio as function of expulsion time for two wall thicknesses. Hemisphere injector; inlet gas temperature, 281±15 K (506°±27° R); tank pressure, 34.47x10^4 newtons per square meter (50 psia). Curves faired through experimental data.

tank wall thicknesses. The figure indicates that the same percentage of the total energy added to the tank was gained by the tank wall for both tank thicknesses. The absolute value of wall energy gained (table II) by the 0.409 centimeter (0.161 in.) thick tank was approximately 6.3 percent less than the 0.762 centimeter (0.30 in.) thick tank.

The absolute values of increase in ullage energy, liquid heating, and mass transfer are approximately the same (within measurement uncertainty) for the two tank wall thicknesses (see tables I and II). Thus, the 6.5-percent reduction in pressurant requirements when using the 0.409 centimeter (0.161 in.) thick wall tank is almost entirely due to the 6.3 percent reduction in the energy gained by the tank wall.

Figure 27 is a comparison of experimental final wall temperature profiles for the two tank wall thicknesses at the end of approximately 276-second expulsions. The 0.409 centimeter (0.161 in.) thick tank has much higher wall temperatures than the 0.762 centimeter (0.30 in.) thick tank in the upper position of the tank. The reduction in wall mass is nearly compensated for by the increase in wall temperature resulting in a difference in wall energy gain for the two profiles of only 6.3 percent. The percent of the total wall

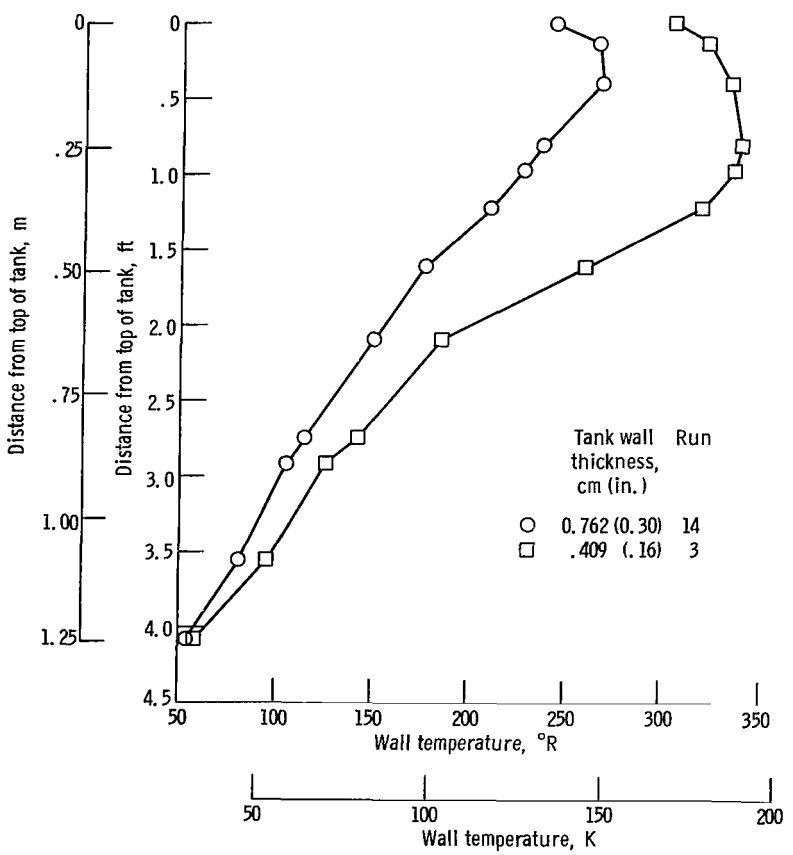

Figure 27. - Comparison of final wall temperature profiles at end of approximately a 276-second expulsion for two tank wall thicknesses. Hemisphere injector; inlet gas temperature, 278±7 K (500°±13° R); tank pressure, 34.47x10^4 newtons per square meter (50 psia).

energy gained by the tank lid for the two tanks was approximately the same (an average of 21 percent of the total was gained by the lid for the thinner wall tank compared with 24 percent gained for the 0.762 cm (0.30 in.) thick tank) even though the lid, for the thinner tank, represented a greater percent of the total tank weight (30 percent compared to 22 percent for the thicker tank). The reason for this was that the initial lid temperature for the thinner tank was an average of 30 K (54° R) higher than the thicker tank prior to expulsion.

For the range of expulsion times investigated herein, the reduction of the wall thickness (tank mass) of 29.5 percent resulted in lowering the pressurant gas requirement by 6.5 percent (11 percent when corrected for inlet gas temperature). For long duration expulsions where the final wall and ullage gas temperatures are dependent on inlet gas temperature and not tank wall mass, the reduction in pressurant requirements would be nearly proportional to the reduction in tank mass (due to a reduction in wall heat capacity).

Effects of ramp rates, inlet gas temperature, and initial ullage volume on the pressurant required to pressurize the tank from atmosphere to 34.47×10^4 newtons per square meter (50 psia). - The amount of pressurant gas needed to initially pressurize a propellant tank may be important for certain missions. This is particularly so for multiburn missions where the tank is vented after each burn or where the coast period between firings is long enough to enable the ullage gas to collapse.

As stated in the INTRODUCTION, the purpose of this investigation was to determine the capability of the analysis to predict the pressurant requirements during the initial pressurization period as well as the expulsion period. For this purpose, data were collected during the initial pressurization period for various pressurizing rates, inlet gas temperatures, and ullage volumes.

Figure 28 is a comparison of the M_I/M_G ratio as a function of inlet gas temperature for two ramp rates at an initial ullage volume of approximately 4 percent. The data were taken using the hemisphere injector. At constant inlet gas temperature, the pressurant requirements decreased for increased ramp rates. The M_I/M_G ratio decreases for increasing inlet gas temperature. The reduced pressurant requirements (for the ramp period) for fast ramp rates using low inlet gas temperature is in agreement with the trends during the expulsion period.

The modification of the analysis of reference 1 for the ramp period is discussed in appendix C. As can be seen in figure 28, the analysis is not capable of accurately predicting the pressurant requirements during the initial pressurization of the 4-percent ullage. However, the prediction of the total pressurant requirement (initial pressurization and expulsion) is still good because the amount of gas required to initially pressurize the 4-percent ullage was only 4.0 percent (maximum) of the pressurant requirement during expulsion.

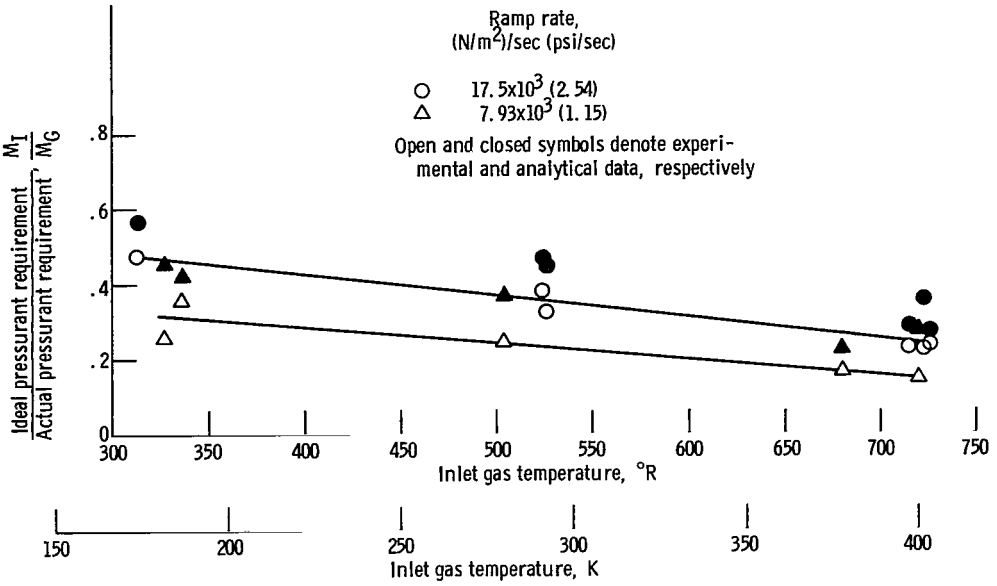

Figure 28. - Comparison of ideal pressurant requirement to actual pressurant requirement ratio as function of inlet gas temperature for two ramp rates at approximately 4-percent ullage volume. Hemisphere injector. Curves faired through experimental data.

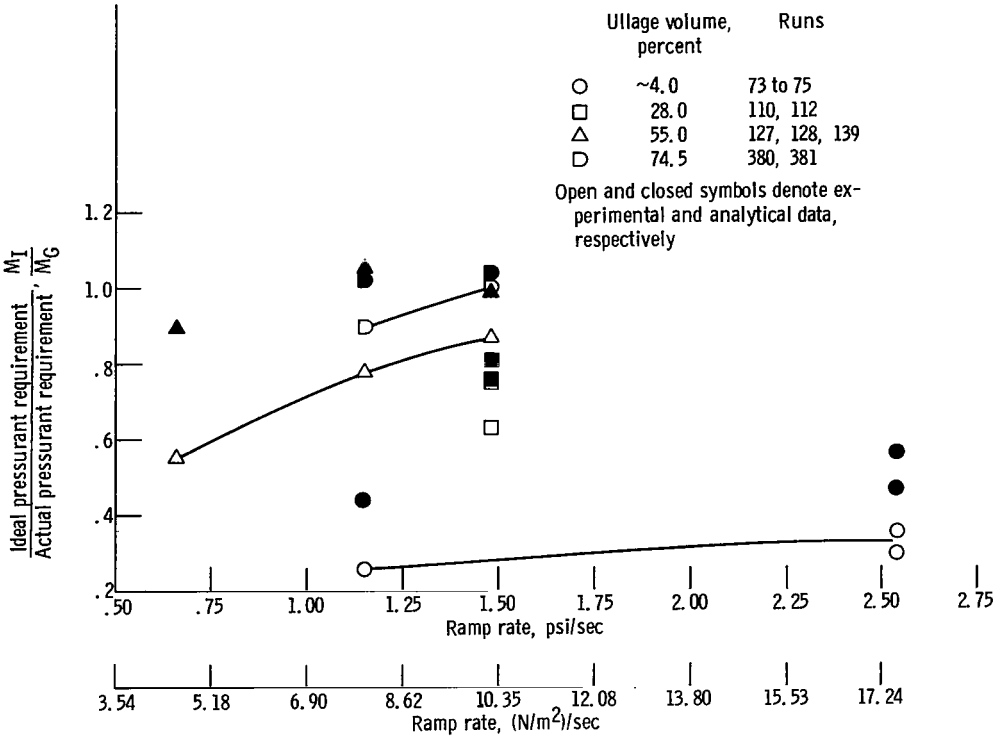

Figure 29. - Comparison of ideal pressurant requirement to actual pressurant requirement ratio as function of ramp rate for various initial ullage volumes. Inlet gas temperature, 167 K (301° R). Curves faired through experimental data.

The absolute perssurant requirements (both experimental and analytical) for the data presented in figures 28 and 29 are given in table IV.

The comparison of M_I/M_G as a function of ramp rate for various initial ullage volumes at an inlet gas temperature of approximately 167 K (301° R) is shown in figure 29. This figure indicates increased M_I/M_G for increased ramp rates for any given initial ullage volume. There is an increased M_I/M_G for the larger ullage volumes for a given ramp rate. Here again, the analysis is not capable of accurately predicting the pressurant requirements. However, the analytical predictions seem to improve for the

TABLE IV. - COMPARISON OF EXPERIMENTAL AND ANALYTICAL VALUES OF PRESSURANT GAS REQUIREMENTS FOR RAMP PERIOD

Run	Initial ullage volume, period	Ramp rate		Mass added				Inlet gas temperature	
		psi/sec	$(N/m^2)/sec$	Experimental		Analysis		°R	K
				lb	kg	lb	kg		
14	8.5	2.54	17.5×10^3	0.108	0.049	0.088	0.040	524	291
17	4.8	2.54	17.5	.068	.031	.049	.022	526	292
60	3.3	1.15	7.93	.068	.031	.048	.022	680	378
61	3.4	1.15	7.93	.075	.034	.047	.021	720	400
64	3.6	2.54	17.50	.048	.022	.037	.017	723	402
65	3.7	↓	↓	.042	.019	.036	.016	726	403
67	5.0			.074	.034	.059	.027	715	397
68	4.0			.057	.026	.036	.016	723	402
69	4.4	1.15	7.93	.086	.039	.057	.026	504	280
70	4.0	1.15	7.93	.062	.028	.053	.024	336	187
71	3.3	2.54	17.50	.087	.039	.059	.027	335	186
73	4.7	2.54	17.50	.078	.035	.066	.030	313	174
74	3.0	2.54	17.50	.073	.033	.056	.025	282	157
75	3.2	1.15	7.93	.086	.039	.049	.022	327	182
110	28.2	1.48	10.20	.365	.166	.286	.130	284	158
112	27.8	1.48	10.20	.302	.137	.298	.135	287	159
127	55.4	1.15	7.93	.593	.269	.436	.198	314	174
128	54.8	.66	4.55	.844	.383	.520	.236	314	174
139	55.6	1.48	10.20	.559	.254	.486	.221	307	171
380	73.5	1.15	7.93	.628	.285	.550	.250	309	172
381	75.4	1.48	10.20	.622	.282	.601	.273	287	159

larger ullage volumes. The transient process that occurs during the initial pressurization of the tank is too complex to be described by the present analytical model. The analytical program can, however, at least be used to predict the approximate magnitude of pressurant requirements during the ramp period.

Concluding remarks. - The comparisons between the analytical and experimental results indicate that for the range of test conditions used, the analytical program and assumptions are adequate to allow prediction of gas requirements during expulsion when using a diffuser type injector. However, the analytical results are not as good when a straight pipe injector is used. The discrepancy is due to substantial amounts of evaporation and to the relatively large radial temperature and velocity gradients existing in the ullage during expulsion when a straight pipe injector is used. The analytical results are very good if compared to the net mass added to the ullage during the expulsion period for all injector geometries.

The analysis is not capable of accurately predicting the pressurant requirements during the initial pressurizing period particularly for small initial ullage volumes. However, since the absolute pressurant requirement for this ramp period for small initial ullage volumes is only a small fraction of the total pressurant required for expulsion, the analysis is considered good enough for approximation.

SUMMARY OF RESULTS

Tank pressurization and propellant expulsion tests were conducted to determine the effect of various physical parameters on the pressurant gas requirements. The experimental results were also compared with predicted results obtained from a previously developed analytical program. The analytical program was revised and extended for these tests conditions. The tests were conducted using two 1.52-meter- (5-ft-) diameter tanks with 0.762 and 0.409 centimeter (0.30 and 0.161 in.) wall thicknesses. The tests were conducted at various inlet gas temperatures, outflow rates, and injector geometries with the following results.

(1) The experimental results indicate decreasing pressurant requirements but decreasing M_I/M_G as the inlet temperature of the pressurizing gas is increased. Of all test variables, inlet temperature had the strongest effect on pressurant gas requirements.

(2) The straight pipe injector had lower pressurant requirements and a greater M_I/M_G than the diffuser type injectors as a result of decreased wall heating, slightly less liquid heating, and increased liquid evaporation. Injector design had the second strongest influence on pressurant gas requirements.

(3) Decreasing the tank mass by 29.5 percent (by decreasing the tank wall thickness from 0.762 to 0.409 cm (0.30 and 0.161 in.)) decreased the pressurant requirements,

increased M_I/M_G, by an average of 6.5 percent (11.0 percent when corrected for variation in inlet gas temperature).

(4) The effects of inlet gas temperature and ramp rate on the pressurant gas required during the initial pressurization of the tank at a 4-percent ullage were as follows:

(a) Increasing inlet gas temperature decreased the pressurant requirement and the M_I/M_G ratio for constant ramp rates.

(b) Increasing ramp rate decreased the pressurant requirement and increases the M_I/M_G ratio for constant inlet gas temperatures.

(5) The trends during the pressurization period for various initial tank ullage volumes and ramp rates are as follows:

(a) Increased pressurant requirement but increased M_I/M_G for larger initial ullage volumes for a constant ramp rate.

(b) Decreased pressurant requirements and increased M_I/M_G for increased ramp rates at a given initial ullage volume.

(6) The ability of the analytical program to predict the experimental results was as follows:

(a) The actual pressurant requirements were predicted within an average of 12.38 percent for all runs (maximum, 21.28 percent; minimum, 6.33 percent). However, the analysis was able to predict the net mass added to the ullage to within an average of 4.93 percent for all runs (maximum 16.7 percent; minimum, 0 percent).

(b) Tank wall heating was predicted within an average of 8.04 percent for all runs with the exception of the straight pipe data which was within 17.29 percent.

(c) Liquid heating was predicted within a minimum of 12.98 percent and a maximum of 31.7 percent for all test conditions.

(d) The analysis failed to predict accurately the pressurant requirements during the initial pressurization of the tank; however, it is considered to be good enough for approximation purposes.

Lewis Research Center,
National Aeronautics and Space Administration,
Cleveland, Ohio, March 7, 1969,
180-31-02-01-22.

APPENDIX A

VARIABLE GEOMETRY, HEAT LOSS TO TANK WALL, AND INTERNAL HARDWARE

The basic analysis used in this report for predicting pressurant gas requirements was developed by W. H. Roudebush in reference 1 for a cylindrical tank.

The major assumptions in the analysis of reference 1 are as follows:

(1) The ullage gas is nonviscous.

(2) The ullage gas velocity is parallel to the tank axis and does not vary radially or circumferentially.

(3) The tank pressure does not vary spatially.

(4) The ullage gas temperature does not vary radially or circumferentially.

(5) The tank wall temperature does not vary radially or circumferentially.

(6) There is no axial heat conduction in either the gas or the wall.

(7) There is no mass transfer (condensation or evaporation).

(8) There is no heat transfer from the pressurant gas to the liquid.

Experiments performed at Lewis (ref. 3) confirmed most of these assumptions. The experimental results indicated, however, that there is significant heat transfer from the gas to the liquid with resulting mass transfer.

For the purposes of this report, the analysis of reference 1 was modified for application to arbitrary symmetric tank shapes, and an attempt was made to incorporate the heat transfer from the gas to the liquid. The treatment of internal hardware (e.g., tank baffles, instrumentation) was also modified to correspond to the treatment of heat transfer to the tank wall.

The primary equations which deal with the pressurizing gas upon entering the tank are

(1) The first law of thermodynamics

(2) The continuity equation

(3) The equation of heat transfer for a point in the tank wall

First Law of Thermodynamics

The form of the first law of thermodynamics used in the analysis in reference 1 for cylindrical tanks is

$$\frac{\partial T}{\partial t} = \frac{2h_c ZRT}{r\overline{M}PC_p}(T_w - T) - \overline{V}\frac{\partial T}{\partial x} + \frac{RTZ_1}{\overline{M}PC_p}\frac{\partial P}{\partial t} + \frac{RTZq_H C_H}{\pi r^2 \overline{M}PC_p}$$

Modifying this equation to account for both arbitrary symmetric tank shapes and internal tank heat sinks gives

$$\frac{\partial T}{\partial t} = \frac{2h_c ZRT}{r\overline{M}PC_p}(T_w - T)\left[1 + \left(\frac{dr}{dx}\right)^2\right]^{1/2} - \frac{\overline{V}\partial T}{\partial x} + \frac{RTZ_1}{\overline{M}PC_p}\frac{\partial P}{\partial t} + \frac{\dot{Q}_H}{C_p M_H} \tag{A1}$$

The first term on the right includes the effect of wall curvature. The last term, the energy lost to the internal hardware, is treated as the summarion of hardware components: (1) laminated thermoplastic, (2) stainless steel, and (3) copper. For the tanks in this investigation,

$$\frac{\dot{Q}_H}{M_H} = \frac{A_1 h_c(T_1 - T)}{\rho V} + \frac{A_2 h_c(T_2 - T)}{\rho V} + \frac{A_3 h_c(T_3 - T)}{\rho V} \tag{A2}$$

where A_1, A_2, and A_3 are effective areas of materials contained within the volume element.

Gluck and Kline, in reference 5, employed the free convection correlation to the pressurant gas (hydrogen, helium) for the pressurized transfer of liquid hydrogen:

$$\frac{h_c L}{k} = Nu = 0.13(GrPr)^{1/3} \tag{A3}$$

This correlation is used herein even though it was developed for cylindrical tanks. Pressurant gas transport properties were evaluated at the mean of the gas and wall temperatures.

Continuity Equation (Area = f(x))

The basic form of the continuity equation for a cylindrical tank is presented in reference 1 (eq. (24)) as

$$\frac{\partial \overline{V}}{\partial x} = \frac{Z_1}{ZT}\left(\frac{\partial T}{\partial t} + \frac{\overline{V}\partial T}{\partial x}\right) - \frac{Z_2}{ZP}\frac{\partial P}{\partial t}$$

The modified form of the continuity equation due to variations in tank radius with distance along the vertical axis becomes

$$\frac{\partial \bar{V}}{\partial x} = \frac{Z_1}{ZT}\left(\frac{\partial T}{\partial t} + \frac{\bar{V}\partial T}{\partial x}\right) - \frac{Z_2}{ZP}\frac{\partial P}{\partial t} - \frac{2\bar{V}}{r}\frac{\partial r}{\partial x} \tag{A4}$$

where Z_1 and Z_2 are defined in reference 1 as

$$Z_1 \equiv Z + T\left(\frac{\partial Z}{\partial T}\right)_P$$

$$Z_2 \equiv Z - P\left(\frac{\partial Z}{\partial P}\right)_T$$

The last term in equation (A4) evolves from the derivation as follows. For the one-dimensional expression for continuity,

$$\frac{\partial}{\partial x}(\rho \bar{V} A) + \frac{\partial}{\partial t}(\rho A) = 0$$

The substitution $A = \pi r^2$ is made where r is the position radius at location x along the vertical axis:

$$\frac{\partial}{\partial x}(\rho \bar{V} r^2) + \frac{\partial}{\partial t}(\rho r^2) = 0$$

The expression for density from the equation of state $\rho = \bar{M}P/ZRT$ is substituted:

$$P\frac{\partial}{\partial x}\left(\frac{\bar{V}r^2}{ZT}\right) + r^2\frac{\partial}{\partial t}\left(\frac{P}{ZT}\right) = 0$$

The following velocity equation is obtained after performing the partial differentiation and after rearranging terms:

$$\frac{\partial \bar{V}}{\partial x} = \left[\frac{1}{T} + \frac{1}{Z}\left(\frac{\partial Z}{\partial T}\right)_P\right]\left(\frac{\partial T}{\partial t} + \frac{\bar{V}\partial T}{\partial x}\right) + \left[\frac{1}{Z}\left(\frac{\partial Z}{\partial P}\right)_T - \frac{1}{P}\right]\frac{\partial P}{\partial t} - \frac{2\bar{V}}{r}\frac{\partial r}{\partial x}$$

When the expressions involving Z_1 and Z_2 are substituted in this equation, equation (A4) is obtained.

Tank Wall Heat Transfer

Reference 1 (eq. (18)) gives the heat-transfer equation which represents the change in wall temperature as a result of the convective process for a cylindrical tank:

$$\frac{\partial T_w}{\partial t} = \frac{h_c}{l_w \rho_w C_w} (T - T_w) + \frac{\dot{q}_w}{l_w \rho_w C_w} \tag{A5}$$

where $\dot{q}_w$ is the rate of heat addition per unit area to the tank wall from outside the tank.

For a small element of volume in the x-direction, equation (A5) can be written as

$$\rho_w C_w V \frac{\partial T_w}{\partial t} = h_c A (T - T_w) + \dot{Q}_w \tag{A6}$$

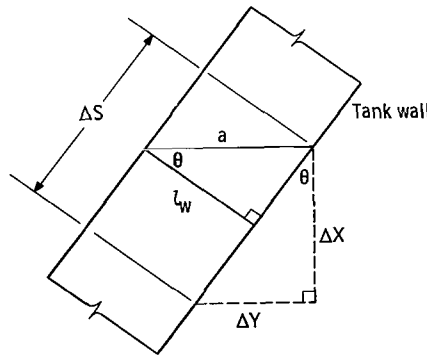

For a wall of arbitrary shape, the following is evident from the sketch:

$$\frac{A}{V} = \frac{2\pi r\, \Delta s}{2\pi r a\, \Delta x} = \frac{\Delta s}{a\, \Delta x} = \frac{1}{l_w}$$

Therefore, equation (A5) holds also for this case.

To account for the large mass concentration at the top of the tank, an equivalent l_w was used. This l_w was obtained by dividing the mass of the tank lid and flange connections by the surface area of the first net point.

APPENDIX B

EQUATIONS OF HEAT AND MASS TRANSFER AT THE GAS-LIQUID INTERFACE

The energy and continuity equations (A1) and (A4) should be modified to incorporate both heat transfer from the ullage gas to the liquid surface and mass transfer into the analysis.

The energy equation should incorporate two additional terms:

(1) The heat-transfer rate from the ullage gas to the liquid interface ($\dot{q}_{U \to S}$)

(2) The energy associated with mass transfer ($\dot{M}_t \lambda$)

Also, the boundary condition at the liquid surface should be revised to account for mass transfer. These additional terms can be related by performing an energy balance at the gas-liquid interface as done by W. A. Olsen in reference 6. The resulting relation, when the interface is saturated, is given by

$$\dot{q}_{U \to S} = \dot{q}_{S \to L} + \frac{\dot{M}_t}{A} \lambda$$

$$= \dot{q}_{S \to L} + \frac{\dot{M}_t}{A} (h_{VAPOR} - H_L) \tag{B1}$$

However, mass transfer was neglected since experimental data, presented in this report, indicate that the mass transfer rate $\dot{M}_t$ was relatively small for most cases (and hence, the energy associated with the mass transferred is small in comparison to $\dot{q}_{S \to L}$). The assumption was made that

$$\dot{q}_{U \to S} = \dot{q}_{S \to L} + \frac{\dot{M}_t}{A} (h_{VAPOR} - h_L) \cong \frac{d}{dt} (U_L) \tag{B2}$$

The term $d/dt(U_L)$ can be determined from experimental data. However, for the purpose of the analysis $\dot{q}_{U \to S}$ must be related to the ullage gas variables. This is done by the relation

$$\dot{q}_{U \to S} \equiv h_{c,L} (T_\delta - T_{sat}) \tag{B3}$$

The flow process is free convection flow of pressurant gas down the tank wall and then radially inward across the liquid surface.

The term T_{sat} was defined by the thermodynamic assumption of local equilibrium for a pure system with relatively small gradients as the saturation temperature corresponding to the tank pressure.

With regard to $h_{c,L}$, reference 7 developed an equation from boundary layer theory for forced flow across a horizontal, semi-infinite, constant temperature flat plate given by

$$Nu = \frac{h_{c,L}L}{k} = 0.664\left(\frac{\mu C_p}{k}\right)^{1/3}\left(\frac{L\overline{V}_L\rho}{\mu}\right)^{1/2} \tag{B4}$$

The velocity $\overline{V}_L$ of the gas across the liquid surface in terms of the gas velocity $\overline{V}_G$ down a vertical wall is given in reference 8 as

$$\overline{V}_L = 0.0975\,\overline{V}_G \tag{B5}$$

where $\overline{V}_G$, obtained by solving the integrated energy and momentum equations at the wall boundary, is given by

$$\overline{V}_G = 1.185\,\frac{\mu}{\rho Z}\,\frac{Gr^{1/2}}{\left[1 + 0.494\,(Pr)^{2/3}\right]^{1/2}} \tag{B6}$$

Combining equations (B5) and (B6) for $\overline{V}_L$ and substituting into (B4) give

$$Nu = \frac{h_{c,L}L}{k} = \frac{0.226\,(Pr)^{1/3}(Gr)^{1/4}}{\left[1 + 0.494\,(Pr)^{2/3}\right]^{1/4}} \tag{B7}$$

Equation (B7) shows that the conductance $h_{c,L}$ across the gas-liquid interface is similar in form to the empirical relation for free convection flow given in reference 9 as

$$Nu = \frac{h_{c,L}L}{k} = 0.14(GrPr)^n \tag{B8}$$

This equation with a value of $n = 1/3$, although somewhat arbitrary, is used in this investigation.

At this point, some choice of T_δ, which is consistent with the definition of $h_{c,L}$ and fits the data for $\dot{q}_{U \to S}$, (i.e., $d/dt(U_L)$) must be made.

In reference 10, which involved the pressurization of hydrogen with a low mixing diffuser and no liquid outflow, the adiabatic compression temperature given by $T_{ad} = T_o (P/P_o)^{(\gamma-1)/\gamma}$ was used as the choice for T_δ. This relation gave good agreement between analytical and experimental mass flux results.

However, for the conditions described in reference 10, appreciable condensation occurred. For greater ullage gas mixing (due to diffuser characteristics as well as the liquid outflow process), T_δ would be expected to be a higher value than T_{ad}. Reference 10 indicated that as T_δ increases these is a tendency toward evaporation - that is, away from the condensation results that occurred when the adiabatic temperature was used.

For the work described herein, T_δ was evaluated using the relation $\dot{q}_{U \to S} = h_{c,L}(T_\delta - T_{sat}) = d/dt\ (U_L)$ for a specific case. The value $d/dt\ (U_L)$ was determined from an experimental run where the expulsion time was approximately 295 seconds. For this condition T_δ was determined to be 1.5 times the adiabatic temperature, or approximately 53 K (95° R), for a tank pressure of 34.47×10^4 newtons per square meter (50 psia). This value of T_δ was used for all comparisons since most of the experimental ullage gas temperature profiles indicated a change in slope around 56 K (101° R).

Using equation (B8), as well as the values for T_δ and T_{sat} discussed above, gave the final form of the equation used to evaluate the heat transferred from the ullage gas to the liquid interface as follows:

$$\dot{q}_{U \to S} = \frac{k}{L}(0.14)(GrPr)^{1/3}(53\ K - T_{sat}) \tag{B9}$$

In order to incorporate liquid heating to the analysis, the term

$$-\frac{\dot{q}_{U \to S} A_L}{X_n V_\rho} \quad \text{or} \quad -\frac{k(0.14)(GrPr)^{1/3}(53\ K - T_{sat})A_L}{L X_n V_\rho} \tag{B10}$$

must be added to the right side of equation (A1).

APPENDIX C

RAMP ANALYSIS

An application of the work reported in reference 1 is the prediction of mass of pressurant for the ramp and hold period. A separate computer program which determines mass of pressurant as well as the tank wall energy requirements during the ramp and hold period is described herein. The same equations which deal with the expulsion period, as outlined in appendix A, are still applicable in the ramp and hold analysis to predict mass of pressurant and wall energy requirements. This analysis computes the gas temperatures in the ullage at any time during the pressure rise from the gas energy equation. The corresponding gas velocities are computed from the equation of continuity. The iterative method to be described shows how convergence is achieved in the solution of the gas energy and continuity equations.

The predicted mass of pressurant is based on an integration of the volume elements in the ullage at the end of the ramp and hold periods.

Because of the complexity of the equations involved in the iteration and because of the small amounts of pressurant required for the ramp when compared with the expulsion, no mass transfer or energy to the liquid is included in this analysis. Mass transfer requirements accounted for approximately 10 percent of the experimental pressurant requirements for the ramp period. Quantitatively, the entire mass of pressurant requirements for the ramp period was less than the expulsion period by a factor of 30 to 60 when the initial ullage was 5 percent of the tank volume.

INPUT DATA REQUIREMENTS

For the solution to proceed, a set of boundary and initial conditions are required. These conditions, which are the same for the expulsion as well as the pressurization, are as follows:

(1) At time $t = 0$, the values of gas temperature T and wall temperature T_W as functions of x, the position within the ullage

(2) On the boundary $x = 0$, the value of inlet gas temperature T as a function of time

(3) At the liquid surface, the value of gas temperature T, wall temperature T_W, and velocity $\overline{V}$ as functions of time (Although movement of the interface has been noted during the ramp pressurization period, no significant effect on the programmed output was noted with the value of $\overline{V} = 0$ at the interface.)

(4) Tank pressure P, outside heating rate $\dot{q}_W$, and inside hardware heating rate $\dot{q}_H$ as functions of time (Like the other initial conditions, the pressure P as a function of time or ramp pressure curve is defined by a discrete set of points which approximate a smooth curve. In regions or pronounced curvature, more points are needed for accurate definition than for linear portions.)

(5) Constant value of heat transfer coefficient h_c, or a correlating equation from which h_c may be evaluated at each net point from values of T, T_W, and P

(6) Tank radius as a function of axial distance down from the top of the tank

(7) Tank wall material properties: density ρ_w and specific heat $C_W(T_W)$

(8) Tank wall thickness (average membrane plus weld area thickness) as a function of axial distance down from the top of the tank

(9) Pressurizing gas properties: molecular weight $\overline{M}$, specific heat $C_p(T)$, and compressibility factor Z(P, T)

(10) Initial ullage height, total time of run, the number of net points in the initial ullage space

(11) The initial time step Δt used in following the pressure rise as well as establishing the points of computation

(12) If the hold period is to be included in the analysis, then the time for the end of the ramp must be specified

APPLICATION OF BASIC EQUATIONS

Reference 1 makes the substitution of $T_{w,i}$ from the finite difference form of (A6) into the finite difference form of the first law. Rearranging gives a quadratic in the gas temperature T_i' where the prime refers to a step forward in time and the quantities without the prime are evaluated at the previous time step:

$$T_i'^2 + \left[\alpha_i^*\left(1 + \overline{V}_i^* \frac{\Delta t}{\Delta x} - \omega_i^*\right) - T_{w,i} - \left(\frac{\dot{q}_w \Delta t}{l_w \rho_w C_w}\right)_i^*\right] T_i' - \alpha_i^*\left(\overline{V}_I^* \frac{\Delta t}{\Delta x} T_{i-1}' + T_i\right) = 0 \qquad \text{(C1)}$$

The quantity marked with the asterisk may be evaluated either at the beginning or the end of the time interval.

A difficulty can arise when evaluating the gas energy equation expressed by the previous quadratic. This occurs when the heat transfer takes place from the wall into the ullage gas. For this situation, the solution of the continuity equation provided negative gas velocities which made it impossible for equation (C1) to converge on the real roots.

At the start of the ramp (immediately after filling the tank), the initial wall temperature distribution in the ullage is higher than the gas temperature distribution. This is brought about since the wall surface above the liquid is exposed to the ambient temperature. But the ullage gas temperature near the liquid interface is close to the saturation temperature at one atmosphere.

The technique used when $T_{w,i} > T_i$ involved a direct substitution. The finite difference form of equation (A4) is

$$\overline{V}'_i = \frac{\left[T'_i \overline{V}'_{i+1} - \left(\frac{Z_1}{Z}\right)'_i \left(\frac{\Delta x}{\Delta t}\right)(T'_i - T_i) + \left(\frac{Z_2}{Z}\right)'_i \frac{T'_i}{P'} \frac{\Delta x}{\Delta t} (P' - P)\right]}{T'_i + \left(\frac{Z_1}{Z}\right)'_i (T'_{i+1} - T'_i) - 2 \frac{\Delta x}{r_i} T'_i \left(\frac{\Delta r}{\Delta x}\right)} \qquad \text{(C2)}$$

Substituting this value of $\overline{V}'_i$ for $\overline{V}^*_i$ in equation (C1) results in the following cubic equation:

$$b_i T'^3_i + \left[\left(\frac{Z_1}{Z}\right)'_i T'_{i+1} + b_i c_i + \alpha^*_i \frac{\Delta t}{\Delta x} (\overline{V}'_{i+1} + d_i)\right] T'^2_i + \left[c_i \left(\frac{Z_1}{Z}\right)'_i T'_{i+1}\right.$$

$$\left. + \alpha^*_i \frac{\Delta t}{\Delta x} \left(\frac{Z_1}{Z}\right)'_i \frac{\Delta x}{\Delta t} T_i - \alpha^*_i \frac{\Delta t}{\Delta x} T'_{i-1}(\overline{V}'_{i+1} + d_i) - \alpha^*_i T_i \frac{\Delta t}{\Delta x} b_i\right] T'_i$$

$$- \alpha^*_i \frac{\Delta t}{\Delta x} \left(\frac{Z_1}{Z}\right)'_i \frac{\Delta x}{\Delta t} T_i T'_{i-1} - \alpha^*_i T_i \left(\frac{Z_1}{Z}\right)'_i T'_{i+1} = 0 \qquad \text{(C3)}$$

This cubic equation is solved for the gas temperature T'_i.

ANALYTICAL PROCEDURE

The analytical procedure uses a variable time increment Δt in following the pressure rise. With this technique, the iteration was stable over a range of inlet conditions and the results were consistent with the recorded data. The iteration proceeds in the following manner. A flow diagram is shown in figure 30 for reference.

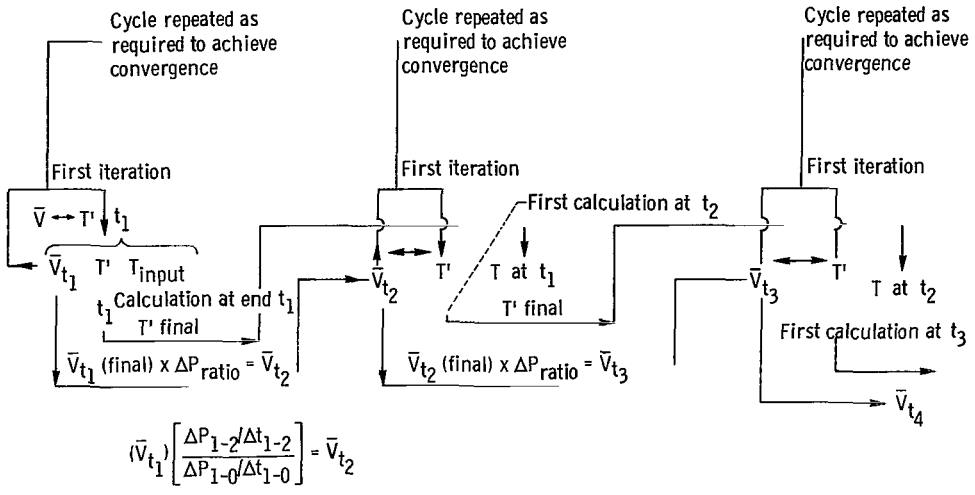

Figure 30. - Flow diagram showing temperature-velocity iteration in energy and continuity equations.

The initial velocity distribution is determined at time $t = 0$ by substituting the initial values of dT/dt from equation (A1) into equation (A4). For all the ramp runs encountered in this investigation, an initial time increment of 1 second proved satisfactory.

TEMPERATURE CALCULATIONS FROM TOP TO INTERFACE

Since values of $\bar{V}$ have been obtained at each net point at time $t = T_1 = 0$, attention is turned to equation (C3) which is cubic in T'_i. During the iteration, the cubic equation (C3) is solved for the gas temperature T'_i starting at the point N_2 in figure 31. When this equation is first solved for the ullage temperature distribution, a value for T'_{i+1} is not available. A substituted value of T_{i+1} proved to be satisfactory as an initial guess to get convergence. All other quantities in equation (C3) are available from the initial conditions. The value for T'_{i-1}, the temperature at N_1, is known as a boundary condition.

The solution for T'_i at N_3 follows, and this procedure continues to calculate gas temperatures until the boundary at the interface is reached. The values for the corresponding wall temperatures are calculated using the finite difference form of equation (A6).

VELOCITY CALCULATIONS FROM INTERFACE TO TOP

Although the ullage temperatures are computed starting at the top (fig. 31), the

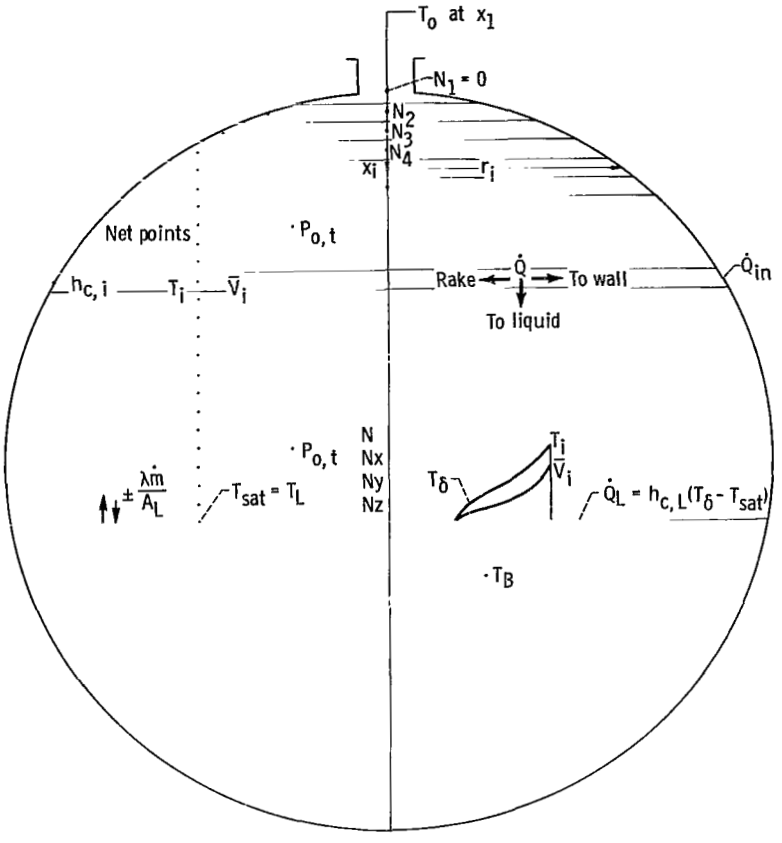

Figure 31. - Analytical model. (Coordinate system is positive in downward direction.)

velocity equation (C2) is used to calculate the ullage gas velocity starting with the point N_y near the interface. The velocity at the interface N_z, the boundary value, is zero with no expulsion.

The ullage gas velocity is calculated from point to point until the top of the tank is reached. The new velocities are used in equation (C3) along with previous values of T'_{i+1} and the temperature distribution is redetermined. This process is continued until convergence is achieved over the entire ullage. The time is then advanced to t_2 and a new set of velocities is determined.

COMPLETING THE SOLUTION

With the new velocities at time t_2, we evaluate equation (C3) again starting at point N_2 and terminating at the interface. A value for T'_{i+1} is always available from the previous iteration, although a substituted value of T_{i+1} is used as the first value.

The new values for T'_i at all the points for time t_2 are used to recompute the velocity distribution. This new set of velocities is then compared with the previous set

and convergence is assumed if the deviation is less than half of 1 percent for every velocity in the time set. A time step is then taken to t_3.

If convergence is not achieved after 40 iterations, the time step is reduced and the iteration process is reinitiated. Generally the reduction in time step becomes necessary only when there is a severe change in the slope of the ramp curve particularly in the early stages of the pressure rise.

For the new time t_3, the temperature T_i' in equation (C3) is determined from its converged value using the iterative method. This procedure continues to evaluate the gas temperatures and velocity distribution in the ullage for each time step taken in following the rate of pressure in the tank.

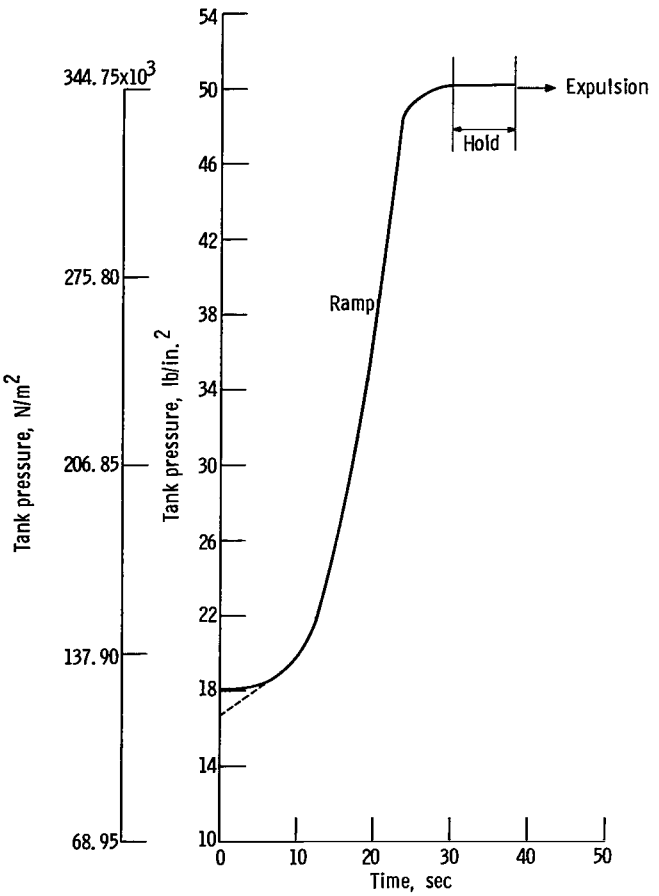

Figure 32. - Tank pressure as function of time during initial pressurization period for run 139.

The initial gas velocity distribution used in solving equation (C3) for each new time t is obtained from the previous time as follows:

$$V_{t,2} = V_{t,1} \frac{\left(\frac{\Delta P_{1-2}}{\Delta t_{1-2}}\right)}{\left(\frac{\Delta P_{0-1}}{\Delta t_{0-1}}\right)} \tag{C4}$$

This iterative procedure can be used for a constant pressure representing the hold period. However, for initiating the ramp, an actual pressure rise must be used. A typical example is shown in figure 32.

REFERENCES

1. Roudebush, William H.: An Analysis of the Problem of Tank Pressurization During Outflow. NASA TN D-2585, 1965.

2. Epstein, M.; Georgius, H. K.; and Anderson, R. E.: A Generalized Propellant Tank Pressurization Analysis. Advanced in Cryogenic Engineering. Vol. 10, Sect. M-U, K. D. Timmerhaus, ed., Plenum Press, 1965, pp. 290-302.

3. DeWitt, Richard L.; Stochl, Robert J.; and Johnson, William R.: Experimental Evaluation of Pressurant Gas Injectors During the Pressurized Discharge of Liquid Hydrogen. NASA TN D-3458, 1966.

4. Stochl, Robert J.; and DeWitt, Richard L.: Temperature and Liquid-Level Sensor for Liquid-Hydrogen Pressurization and Expulsion Studies. NASA TN D-4339, 1968.

5. Gluck, D. F.; and Kline, J. F.: Gas Requirements in Pressurized Transfer of Liquid Hydrogen. Advances in Cryogenic Engineering. Vol. 7, K. D. Timmerhaus, ed., Plenum Press, 1962, pp. 219-233.

6. Olsen, William A.: Analytical and Experimental Study of Three Phase Heat Transfer with Simultaneous Condensating and Freezing on Cold Horizontal and Vertical Plates. Ph. D. Thesis, Univ. Connecticut, 1967.

7. Kays, W. M.: Convective Heat and Mass Transfer. McGraw-Hill Book Co., Inc., 1966.

8. Dickson, Philip F.: Large Gradient Mass Transfer. Ph. D. Thesis, Univ. Minnesota, 1962.

9. McAdams, William H.: Heat Transmission. Third ed., McGraw-Hill Book Co., Inc., 1954.

10. Olsen, William A.: Experimental and Analytical Investigation of Interfacial Heat and Mass Transfer in a Pressurized Tank Containing Liquid Hydrogen. NASA TN D-3219, 1966.

NASA-Langley, 1969 —— 28 E-4676

NATIONAL AERONAUTICS AND SPACE ADMINISTRATION
WASHINGTON, D.C. 20546
OFFICIAL BUSINESS

FIRST CLASS MAIL

POSTAGE AND FEES PAID
NATIONAL AERONAUTICS AND
SPACE ADMINISTRATION

POSTMASTER: If Undeliverable (Section 158 Postal Manual) Do Not Return

"The aeronautical and space activities of the United States shall be conducted so as to contribute . . . to the expansion of human knowledge of phenomena in the atmosphere and space. The Administration shall provide for the widest practicable and appropriate dissemination of information concerning its activities and the results thereof."

— NATIONAL AERONAUTICS AND SPACE ACT OF 1958

NASA SCIENTIFIC AND TECHNICAL PUBLICATIONS

TECHNICAL REPORTS: Scientific and technical information considered important, complete, and a lasting contribution to existing knowledge.

TECHNICAL NOTES: Information less broad in scope but nevertheless of importance as a contribution to existing knowledge.

TECHNICAL MEMORANDUMS: Information receiving limited distribution because of preliminary data, security classification, or other reasons.

CONTRACTOR REPORTS: Scientific and technical information generated under a NASA contract or grant and considered an important contribution to existing knowledge.

TECHNICAL TRANSLATIONS: Information published in a foreign language considered to merit NASA distribution in English.

SPECIAL PUBLICATIONS: Information derived from or of value to NASA activities. Publications include conference proceedings, monographs, data compilations, handbooks, sourcebooks, and special bibliographies.

TECHNOLOGY UTILIZATION PUBLICATIONS: Information on technology used by NASA that may be of particular interest in commercial and other non-aerospace applications. Publications include Tech Briefs, Technology Utilization Reports and Notes, and Technology Surveys.

Details on the availability of these publications may be obtained from:

SCIENTIFIC AND TECHNICAL INFORMATION DIVISION

NATIONAL AERONAUTICS AND SPACE ADMINISTRATION

Washington, D.C. 20546